Supplementary Document of "Two-Archive Evolutionary Algorithm for Constrained Multi-Objective Optimization"[*]

Ke Li[#1], Renzhi Chen[#3], Guangtao Fu[4] and Xin Yao[2,3]

[1]Department of Computer Science, University of Exeter
[2]Department of Computer Science and Engineering, Southern University of Science and Technology
[3]CERCIA, School of Computer Science, University of Birmingham
[4]Department of Engineering, University of Exeter
[*]Email: {k.li, g.fu}@exeter.ac.uk, rxc332@cs.bham.ac.uk, xiny@sustc.edu.cn
[#]The first two authors make equal contributions to this paper.

1   Constrained Test Problems

This section provides the detailed descriptions of the constrained test problems used in our empirical studies. In particular, we mainly describe the mathematical formulations and characteristics of the constraints while the baseline test problems are from the classic DTLZ benchmark suite [1]. Note that this benchmark suite has been extensively used in the evolutionary multi-objective optimisation community [2–23]. We start from C-DTLZ problems proposed in [24], followed by DC-DTLZ problems developed by us.

1.1   C-DTLZ Benchmark Suite

1.1.1   Type-1 Constrained Problems

Here the original Pareto front (PF) is kept the same, but there is an infeasible barrier that causes difficulties for an algorithm in converging toward the PF. C1-DTLZ1 is defined as:

$$\left.\begin{aligned}
\min f_1(\mathbf{x}) &= \frac{1}{2}x_1 x_2 \cdots x_{m-1}(1 + g(\mathbf{x}_m)), \\
\min f_2(\mathbf{x}) &= \frac{1}{2}x_1 x_2 \cdots (1 - x_{m-1})(1 + g(\mathbf{x}_m)), \\
&\vdots \\
\min f_{m-1}(\mathbf{x}) &= \frac{1}{2}x_1(1 - x_2)(1 + g(\mathbf{x}_m)), \\
\min f_m(\mathbf{x}) &= \frac{1}{2}(1 - x_1)(1 + g(\mathbf{x}_m))
\end{aligned}\right\} \tag{1}$$

where

$$g(\mathbf{x}_m) = 100\Big[|\mathbf{x}_m| + \sum_{x_i \in \mathbf{x}_m}(x_i - 0.5)^2 - \cos(20\pi(x_i - 0.5))\Big], \tag{2}$$

and $\mathbf{x}_m = (x_m, \cdots, x_n)^T$. In particular, the constraint is defined as:

$$c(\mathbf{x}) = 1 - \frac{f_m(\mathbf{x})}{0.6} - \sum_{i=1}^{m-1}\frac{f_i(\mathbf{x})}{0.5} \geq 0. \tag{3}$$
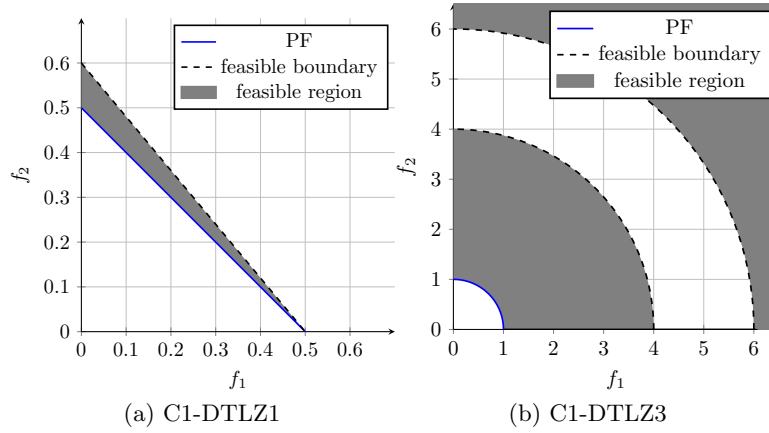
Figure 1: Illustration of the feasible region of C1-DTLZ1 and C1-DTLZ3 in 2-D.

An illustrative example of the feasible region and PF in the 2-objective case is shown in Fig. 1(a).

C1-DTLZ3 is defined as:

$$
\left.\begin{aligned}
\min f_1(\mathbf{x}) &= (1 + g(\mathbf{x}_m)) \cos(x_1\pi/2) \cdots \cos(x_{m-2}\pi/2) \\
&\cos(x_{m-1}\pi/2), \\
\min f_2(\mathbf{x}) &= (1 + g(\mathbf{x}_m)) \cos(x_1\pi/2) \cdots \cos(x_{m-2}\pi/2) \\
&\sin(x_{m-1}\pi/2), \\
\min f_3(\mathbf{x}) &= (1 + g(\mathbf{x}_m)) \cos(x_1\pi/2) \cdots \sin(x_{m-2}\pi/2), \\
&\vdots \\
\min f_m(\mathbf{x}) &= (1 + g(\mathbf{x}_m)) \sin(x_1\pi/2),
\end{aligned}\right\}
\tag{4}
$$

where the $g(\mathbf{x}_m)$ is the same as equation (2), while the constraint is defined as:

$$
c(\mathbf{x}) = (\sum_{i=1}^{m} f_i(\mathbf{x})^2 - 16)(\sum_{i=1}^{m} f_i(\mathbf{x})^2 - r^2) \geq 0.
\tag{5}
$$

In particular, we set $r = \{9, 12.5, 12.5, 15, 15\}$ for $m \in \{3, 5, 8, 10, 15\}$ as recommended in [24]. An illustrative example of the feasible region and PF in the 2-objective case is shown in Fig. 1(b).

1.1.2 Type-2 Constrained Problem

This constraint is designed to introduce infeasibility to some parts of the PF. The objective functions of C2-DTLZ2 are the same as equation (4) but the $g(\mathbf{x}_m)$ is defined as:

$$
g(\mathbf{x}_m) = \sum_{x_i \in \mathbf{x}_m} (x_i - 0.5)^2,
\tag{6}
$$

and the constraint is defined as:

$$
c(\mathbf{x}) = \max \left\{ \max_{i=1}^{m} \left[(f_i(\mathbf{x}) - 1)^2 + \sum_{j=1, j \neq i}^{m} f_j^2 - r^2 \right], \\
\left[\sum_{i=1}^{m} (f_i(\mathbf{x}) - \frac{1}{\sqrt{m}})^2 - r^2 \right] \right\},
\tag{7}
$$

To make this test problem more challenging, we set $r = 0.1$ in our empirical studies. An illustrative example of the feasible region and PF in the 2-objective case is shown in Fig. 2.
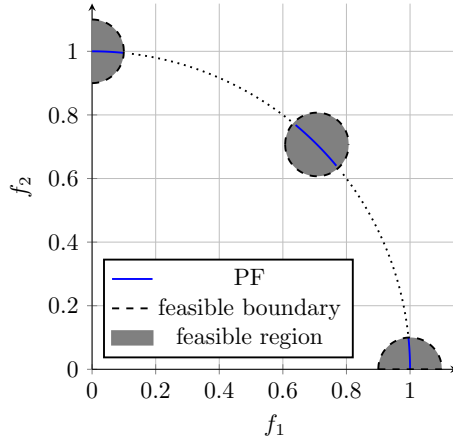

Figure 2: Illustration of the feasible region of C2-DTLZ2 in 2-D.

1.1.3   Type-3 Constrained Problems

These problems involve multiple constraints and the PF is formed by portions of the added constraint surfaces. C3-DTLZ1 has the same objective functions as C1-DTLZ1, but the constraint is defined as:

$$c_j(\mathbf{x}) = \sum_{i=1, i \neq j}^{m} f_j(\mathbf{x}) + \frac{f_j(\mathbf{x})}{0.5} - 1 \geq 0, \forall j = 1, \cdots, m. \tag{8}$$

An illustrative example of the feasible region and PF in the 2-objective case is shown in Fig. 3(a).
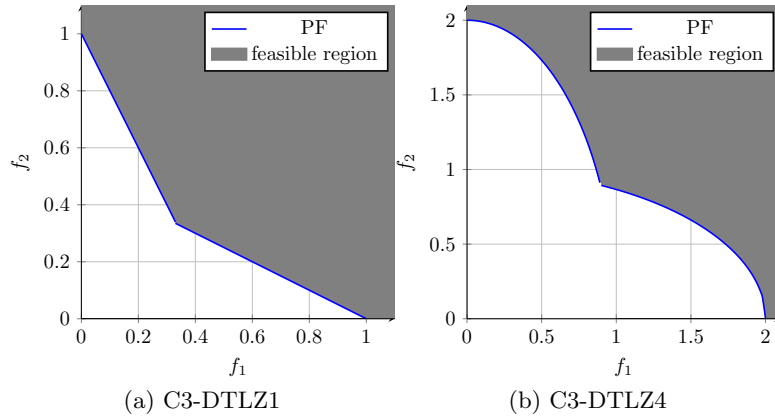

(a) C3-DTLZ1

(b) C3-DTLZ4

Figure 3: Illustration of the feasible region of C3-DTLZ1 and C3-DTLZ4 in 2-D.

C3-DTLZ4 is defined as:

$$\left.\begin{aligned}
\min f_1(\mathbf{x}) &= (1 + g(\mathbf{x}_m)) \cos(x_1^\alpha \pi/2) \cdots \cos(x_{m-2}^\alpha \pi/2) \\
&\cos(x_{m-1}^\alpha \pi/2), \\
\min f_2(\mathbf{x}) &= (1 + g(\mathbf{x}_m)) \cos(x_1^\alpha \pi/2) \cdots \cos(x_{m-2}^\alpha \pi/2) \\
&\sin(x_{m-1}^\alpha \pi/2), \\
\min f_3(\mathbf{x}) &= (1 + g(\mathbf{x}_m)) \cos(x_1^\alpha \pi/2) \cdots \sin(x_{m-2}^\alpha \pi/2), \\
&\vdots \\
\min f_m(\mathbf{x}) &= (1 + g(\mathbf{x}_m)) \sin(x_1^\alpha \pi/2),
\end{aligned}\right\} \tag{9}$$

where

$$g(\mathbf{x}_m) = \sum_{x_i \in \mathbf{x}_m} (x_i - 0.5)^2. \tag{10}$$

3

In particular, the constraints are defined as:

$$c_j(\mathbf{x}) = \frac{f_j^2}{4} + \sum_{i=1, i \neq j}^{m} f_i(\mathbf{x})^2 - 1 \geq 0, \forall j = 1, \cdots, m. \tag{11}$$

An illustrative example of the feasible region and PF in the 2-objective case is shown in Fig. 3(b).

1.2 DC-DTLZ Benchmark Suite

Different from C-DTLZ benchmark suite, in which the constraints act on the objective space, DC-DTLZ benchmark suite, developed in this paper, have constraints act on the decision space. Similar to Section 1.1, we develop three different types of constraints as follows.

1.2.1 Type-1 Constrained Problems

Similar to the Type-2 constrained problem of the C-DTLZ benchmark suite, the constrained problems introduced here also aim to introduce several infeasible segments on the PF. Specifically, DC1-DTLZ1 and DC1-DTLZ3 have the same objective functions as C1-DTLZ1 and C1-DTLZ3, but their corresponding constraints are defined as:

$$c(\mathbf{x}) = \cos(a\pi * x_1) > b, \tag{12}$$

In particular, $a > 0$ controls the number of feasible segments on the PF. Note that each feasible segment is a cone starting from the origin, as shown in Fig. 4(a) and Fig. 4(b). $0 < b < 1$ controls the size of each feasible segment, where a large b leads to a narrow feasible segment. In our empirical studies, we set $a = 3$ and $b = 0.5$.
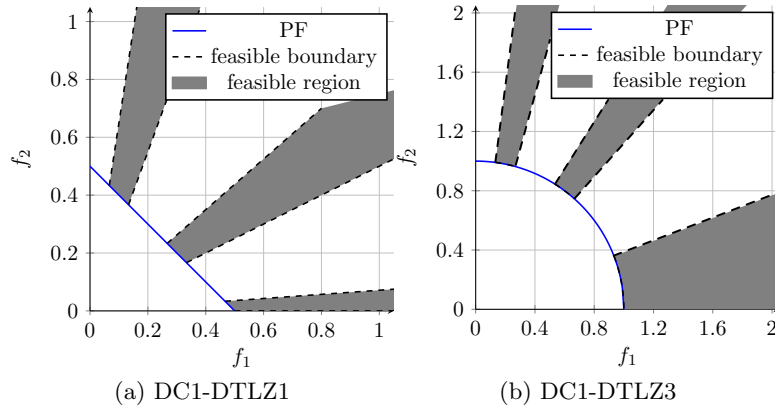

Figure 4: Illustration of the feasible region of DC1-DTLZ1 and DC1-DTLZ3 in 2-D.

1.2.2 Type-2 Constrained Problem

Similar to the Type-1 constrained problem of the C-DTLZ benchmark suite, the constrained problems introduced here have the same PF as the baseline test problems. But the constraints make most of the attainable objective space become infeasible as shown in Fig. 5(a) and Fig. 5(b). Specifically, DC2-DTLZ1 and DC2-DTLZ3 have the same objective functions as C1-DTLZ1 and C1-DTLZ3, while there are two constraints defined as:

$$c_1(\mathbf{x}) = cos(a\pi g(\mathbf{x}_m)) > b, \tag{13}$$

and

$$c_2(\mathbf{x}) = e^{-g(\mathbf{x}_m)} > b. \tag{14}$$

It is worth noting that the constraint violation (CV) of a solution $\mathbf{x}$ fluctuates with the decrease of $g(\mathbf{x}_m)$, as shown in Fig. 6. In other words, $CV(\mathbf{x})$ does not monotonically decreases when it converges
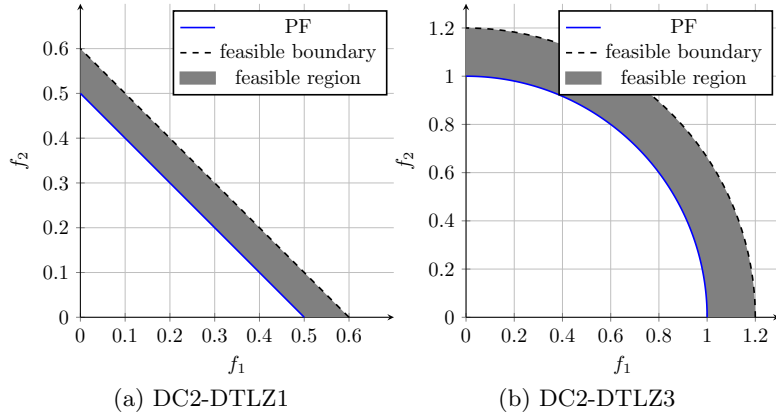
(a) DC2-DTLZ1 (b) DC2-DTLZ3

Figure 5: Illustration of the feasible region of DC2-DTLZ1 and DC2-DTLZ3 in 2-D.

toward the PF, while there exists several local optima of CV which can obstruct the convergence of $\mathbf{x}$. In particular, $a > 0$ controls the number of local optima of CV, while $0.5 < b < 1$ controls the value of the corresponding local optimum.
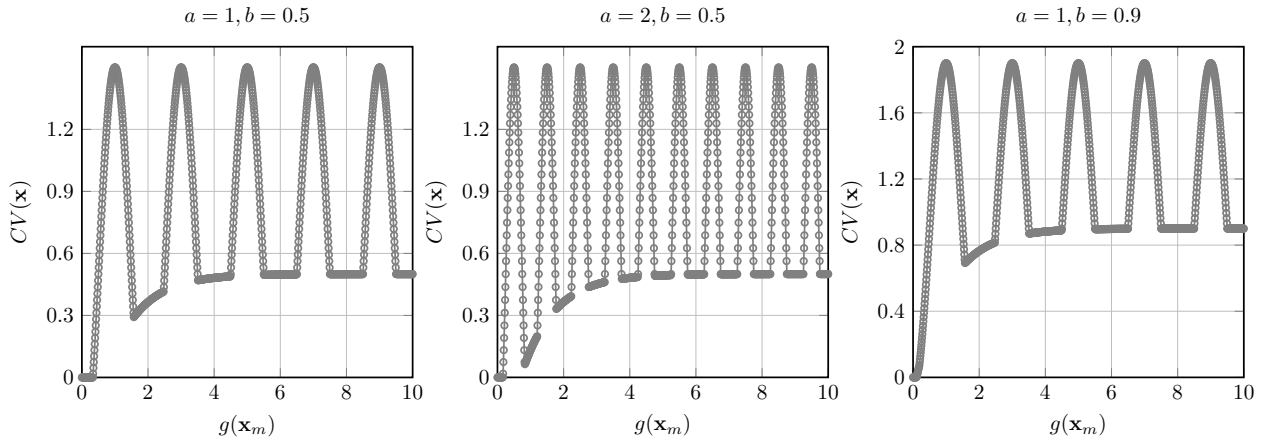

Figure 6: Variation of $CV(\mathbf{x})$ with respect to $g(\mathbf{x})$.

1.2.3 Type-3 Constrained Problem

This type of constrained problem is a combination of Type-1 and Type-2 constraints. The objective functions of DC3-DTLZ1 and DC3-DTLZ3 are the same as before, while the $m + 1$ constraints are defined as:

$$c_j(\mathbf{x}) = \cos(a\pi x_j) > b, \forall j = 1, \cdots, m, \tag{15}$$

and

$$c_{m+1}(\mathbf{x}) = \cos(a\pi g(\mathbf{x}_m)) > b. \tag{16}$$

As shown in Fig. 7(a), similar to DC1-DTLZ1, the PF of DC3-DTLZ1 is partially feasible. In particular, the shape of the infeasible region is similar to that of DC1-DTLZ1 but is cut into several feasible segments. In addition, similar to DC2-DTLZ1, there exists several local optima of CV which are away from the PF. In particular, $a > 0$ controls the gap between different feasible segment along the same cone while $0.5 < b < 1.0$ controls the size of each feasible segment. Fig. 7(b) shows the feasible region and the PF of DC3-DTLZ3. Its property is similar to that of DC3-DTLZ1.
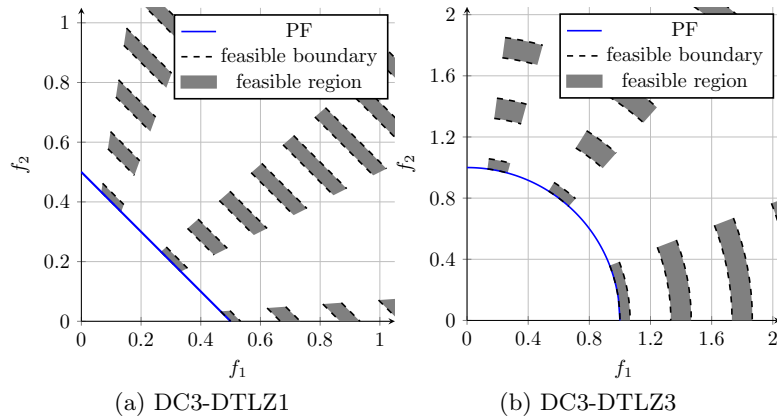
(a) DC3-DTLZ1　　　　　(b) DC3-DTLZ3

Figure 7: Illustration of the feasible region of DC3-DTLZ1 and DC3-DTLZ3 in 2-D.

1.3   Comparison of Feasible Ratio

In Table 1 and Table 2, we presented the feasible ratios of different test problems. In particular, the feasible ratio is an estimated size of the feasible region with respect to the whole search space. To estimate this quantity, for a test problem, we randomly sampled 10^7 solutions, according to a uniform distribution, in the corresponding decision space, while the feasible ratio is the percentage of those feasible solutions. However, due to the non-uniform mapping between the decision space and the objective space, a uniform sampling in the decision space can hardly lead to the corresponding uniform samples in the objective space. For example, although the feasible ratio of C1-DTLZ3 is always 100%, the sampled feasible solutions are all in the outer feasible segment. The infeasible barrier, as shown in Fig. 1(b), still plays as a significant obstacle to overcome. As for C3-DTLZ4, the objective values of a randomly initialized solution can only fall in the range $[1, 2.5]$. This explains its low feasible ratio.

Table 1: Feasible ratios of C-DTLZ benchmark problems

Problem	m				
	3	5	8	10	15
C1-DTLZ1	0.00%	0.00%	0.00%	0.00%	0.00%
C1-DTLZ3	100.00%	100.00%	100.00%	100.00%	100.00%
C2-DTLZ2	0.00%	0.00%	0.00%	0.00%	0.00%
C3-DTLZ1	100.00%	100.00%	100.00%	100.00%	100.00%
C3-DTLZ4	1.84%	3.16%	5.09%	6.38%	9.48%

Table 2: Feasible ratios of DC-DTLZ benchmark problems

Problem	m				
	3	5	8	10	15
DC1-DTLZ1	10.11%	10.12%	10.11%	10.10%	10.12%
DC1-DTLZ3	10.11%	10.11%	10.13%	10.11%	10.11%
DC2-DTLZ1	0.00%	0.00%	0.00%	0.00%	0.00%
DC2-DTLZ3	0.00%	0.00%	0.00%	0.00%	0.00%
DC3-DTLZ1	3.70%	0.41%	0.02%	0.00%	0.00%
DC3-DTLZ3	3.70%	0.41%	0.02%	0.00%	0.00%

2 Algorithms for Comparisons

In our empirical studies, we choose five state-of-the-art constrained evolutionary multi-objective optimization (EMO) algorithms for peer comparisons. We briefly describe their basic ideas as follows:

- C-MOEA/D [24]: It is a modification of the MOEA/D-DE developed in [25], where the feasibility information is incorporated in the update procedure: 1) if the offspring is feasible while the parent is infeasible, the offspring will replace this parent; otherwise, the parent survives; 2) if both offspring and parent are infeasible, the one having the smaller CV survives; 3) if both of them are feasible, we compare the aggregation function value as usual.

- C-NSGA-III [24]: It is a modification of NSGA-III [26] where the Pareto dominance relation is replaced with the constrained dominance relation.

- C-MOEA/DD [11]: It is our recently developed algorithm that incorporates the Pareto dominance and decomposition into a single paradigm. Similar to NSGA-II, we first divide the population into several non-domination levels, and solutions in the first several levels have a higher priority to survive to the next generation. Afterwards, the exceeded solutions are trimmed according to the density information of their associated subregion and their aggregation function values. To improve the population diversity, an infeasible solution can survive to the next generation in case it is in an isolated subregion.

- I-DBEA [27]: It is a decomposition-based evolutionary algorithm where the balance between convergence and diversity is maintained by two independent distance measures and a simple preemptive distance comparison scheme for solution association. In addition, I-DBEA uses an adaptive epsilon formulation to deal with constraints.

- CMOEA [28]: It uses an adaptive penalty function and a distance measure to handle constraints. In particular, these two functions are developed upon the objective function values and the sum of CVs of each solution. By doing so, the original constrained multi-objective optimization problem (MOP) is transformed to a unconstrained format. In particular, the corresponding objective functions take account of both the optimality and feasibility. Afterwards, the classic NSGA-II is used to optimize this newly formed unconstrained MOP.

All algorithms use the simulated binary crossover [29] and the polynomial mutation [30] for offspring generation. The corresponding parameters are set in Table 3.

Table 3: Parameter settings for reproduction operators

Parameter	Setting
crossover probability p_c	0.9
mutation probability p_m	$\frac{1}{n}$
crossover index μ_c	30
mutation index μ_m	20

The population size is set as shown in Table 4. The termination criteria is the number of function evaluations (FEs) which is presented in Table 5. Note that CMOEA shares the same settings as C-NSGA-III; while the other algorithms share the same settings with C-TAEA. In particular, the setting of weight vectors is based on the method developed in [11].

3 Comparison Results on HV metric for C-DTLZ and DC-DTLZ problems

This section provides the comparison results of the HV values obtained by C-TAEA and the other five peer algorithms on C-DTLZ and DC-DTLZ problems. Please find the detailed information from Table 6 and Table 7.

Table 4: Number of weight vectors and the population size

m	♯ of weight vectors	C-NSGA-III	C-TAEA
3	91	92	91
5	210	212	210
8	156	156	156
10	275	276	275
15	135	136	135

Table 5: Number of FEs of different test instances.

Problem	$m = 3$	$m = 5$	$m = 8$	$m = 10$	$m = 15$
C1-DTLZ1	$500 \times N$	$600 \times N$	$800 \times N$	$1,000 \times N$	$1,500 \times N$
C1-DTLZ3	$1,000 \times N$	$1,500 \times N$	$2,500 \times N$	$3,500 \times N$	$5,000 \times N$
C2-DTLZ2	$250 \times N$	$350 \times N$	$500 \times N$	$750 \times N$	$1,000 \times N$
C3-DTLZ1	$750 \times N$	$1,250 \times N$	$2,000 \times N$	$3,000 \times N$	$4,000 \times N$
C3-DTLZ4	$750 \times N$	$1,250 \times N$	$2,000 \times N$	$3,000 \times N$	$4,000 \times N$

N is the population size used for C-NSGA-III as shown in Table 4.

Table 6: Comparison results on HV metric (median and IQR) for C-TAEA and the other peer algorithms on C-DTLZ benchmark suite

	m	C-TAEA	C-NSGA-III	C-MOEA/D	C-MOEA/DD	I-DBEA	CMOEA
C1-DTLZ1	3	1.3042(1.01E-3)	1.3020(1.89E-3)†	**1.3043(5.43E-4)**	1.3043(1.07E-3)	1.3033(2.42E-4)	1.3039(1.60E-3)
	8	2.1435(3.02E-3)	2.1431(6.59E-4)	2.1436(1.00E-6)	**2.1436(8.00E-6)**	2.1436(6.01E-6)	2.1436(1.35E-6)
	10	2.5937(2.01E-6)	**2.5940(3.52E-4)**	2.5937(1.02E-6)	2.5937(5.11E-6)	2.5937(1.03E-6)	2.5937(2.03E-6)
	15	**4.1022(3.83E-2)**	4.0812(8.86E-2)	4.0072(7.77E-2)†	4.0277(9.15E-2)	4.0911(7.93E-2)	4.0288(3.35E-2)
C1-DTLZ3	3	**0.7351(4.00E-2)**	0.0000(0.00E+0)†	0.0000(0.00E+0)†	0.0000(0.00E+0)†	0.0000(0.00E+0)†	0.0000(0.00E+0)†
	5	**0.1761(1.76E-1)**	0.0000(0.00E+0)†	0.0000(0.00E+0)†	0.0000(0.00E+0)†	0.0000(0.00E+0)†	0.0000(0.00E+0)†
	8	**1.5943(8.54E-2)**	0.0000(0.00E+0)†	0.0000(0.00E+0)†	0.0000(0.00E+0)†	0.0000(0.00E+0)†	0.0000(0.00E+0)†
	10	**2.5132(6.34E-1)**	0.0000(0.00E+0)†	0.0000(0.00E+0)†	0.0000(0.00E+0)†	0.0000(0.00E+0)†	0.0000(0.00E+0)†
	15	**2.1825(3.86E-2)**	0.0000(0.00E+0)†	0.0000(0.00E+0)†	0.0000(0.00E+0)†	0.0000(0.00E+0)†	0.0000(0.00E+0)†
C2-DTLZ2	3	**0.4130(2.81E-4)**	0.1225(1.00E-5)†	0.1225(1.11E-1)†	0.0000(1.21E-1)†	0.1225(3.50E-5)†	0.1225(6.50E-5)†
	5	**0.8607(2.50E-1)**	0.1482(3.00E-6)†	0.6117(4.63E-1)†	0.1482(7.30E-3)†	0.1482(6.13E-2)†	0.1482(5.21E-4)†
	8	**1.1426(6.57E-3)**	0.1973(2.90E-5)†	0.1973(3.12E-6)†	0.1949(7.21E-3)†	0.3764(1.79E-1)†	0.1973(2.32E-6)†
	10	**1.5937(2.70E-5)**	0.2387(1.20E-5)†	0.2387(2.03E-1)†	0.2358(7.21E-2)†	0.2386(2.17E-1)†	0.2387(3.71E-6)†
	15	**2.4033(6.90E-2)**	0.3840(5.90E-3)†	0.3843(7.63E-2)†	0.3797(9.26E-2)†	0.3845(5.40E-2)†	0.3843(4.26E-2)†
C3-DTLZ1	3	**1.1515(5.15E-4)**	1.1499(1.46E-2)	1.1253(2.37E-2)†	1.1086(5.30E-4)†	1.1310(3.56E-2)	1.1427(6.03E-6)
	5	**1.5781(2.15E-4)**	1.5736(1.28E-2)	1.5776(7.27E-4)	1.5656(2.20E-5)†	1.5780(1.04E-4)	1.5779(7.30E-5)
	8	2.1386(5.66E-4)	2.1332(3.07E-3)	**2.1386(3.14E-4)**	2.1367(4.00E-6)	2.1385(5.80E-5)	2.1386(9.00E-6)
	10	2.5929(2.20E-5)	2.5890(3.95E-3)	**2.5929(1.50E-5)**	2.5926(1.72E-2)	2.5929(7.36E-2)	2.5929(2.11E-2)
	15	4.1422(3.68E-1)	**4.1769(5.67E-1)**	4.1631(4.29E-2)	4.1701(7.82E-2)	4.1202(5.30E-2)	4.1663(8.62E-2)
C3-DTLZ4	3	8.4280(1.23E-2)	**8.4280(1.16E-3)**	8.4165(6.70E-3)†	8.4161(1.35E-2)†	8.4150(9.29E-2)†	8.4166(8.02E-2)†
	5	**49.5453(2.20E-3)**	49.5451(7.20E-2)	49.5330(5.80E-3)†	49.5327(6.90E-3)†	49.5346(1.67E-2)†	49.5257(3.93E-2)†
	8	546.4971(4.56E-2)	**546.4971(1.10E-3)**	546.4951(4.20E-3)	546.4943(2.29E-2)	546.4933(3.73E-2)	546.4942(4.21E-2)
	10	2654.4042(9.19E-2)	**2654.4042(7.84E-2)**	2654.4042(5.37E-2)	2654.4041(1.98E-2)	2654.4042(3.24E-2)	2654.4042(3.15E-2)
	15	**136803.0202(4.13E-2)**	136802.2201(3.70E-2)†	136802.2302(5.26E-2)†	136802.1233(9.10E-2)†	136802.1921(9.80E-0)†	136802.0201(6.23E-1)†

† denotes the performance of C-TAEA is significantly better than the other peers according to the Wilcoxon's rank sum test at a 0.05 significance level; ‡ denotes the corresponding algorithm significantly outperforms C-TAEA.

Table 7: Comparison results on HV metric (median and IQR) for C-TAEA and the other peer algorithms on DC-DTLZ benchmark suite

	m	C-TAEA	C-NSGA-III	C-MOEA/D	C-MOEA/DD	I-DBEA	CMOEA
DC1-DTLZ1	3	**1.2006(1.70E-2)**	1.1982(9.96E-2)†	0.9631(2.81E-2)†	1.1845(3.05E-2)†	1.1883(9.25E-2)†	1.1883(8.40E-3)†
	5	**1.4783(3.27E-2)**	1.4725(3.36E-2)†	1.4783(5.05E-2)†	1.4762(8.46E-2)†	1.4782(7.29E-2)†	1.4779(3.13E-2)†
	8	**1.9682(1.24E-2)**	1.9347(8.57E-2)†	1.9660(8.95E-2)†	1.9655(5.82E-2)†	1.9678(5.45E-2)†	1.9676(8.14E-2)†
	10	**2.3890(3.67E-3)**	2.3113(4.34E-2)†	2.3792(3.64E-2)†	2.3801(4.30E-3)†	2.3797(7.50E-2)†	2.3810(8.70E-3)†
	15	**4.1012(1.73E-2)**	4.0031(2.76E-2)†	4.0122(1.78E-2)†	4.0823(7.88E-2)†	4.0911(5.84E-2)†	4.0532(4.03E-2)†
DC1-DTLZ3	3	**0.6339(6.51E-2)**	0.5088(7.54E-2)†	0.6694(3.99E-2)†	0.5386(9.32E-2)†	0.4545(6.00E-3)†	0.4545(6.76E-2)†
	5	**1.2656(3.68E-2)**	1.2582(7.39E-2)†	1.1463(1.20E-3)†	1.1712(2.26E-2)†	1.1467(5.86E-2)†	1.1462(9.40E-3)†
	8	**1.9829(5.39E-2)**	1.8461(7.95E-2)†	1.9301(5.70E-2)†	1.9640(4.34E-2)†	1.9284(3.78E-2)†	1.9793(4.67E-2)†
	10	**2.5181(6.01E-2)**	2.3880(9.70E-3)†	2.4903(9.02E-2)†	2.5083(3.17E-2)†	2.4902(4.92E-2)†	2.4986(6.52E-2)†
	15	**4.1700(7.56E-2)**	4.0321(3.01E-2)†	4.0422(2.80E-2)†	4.0282(2.86E-2)†	3.9123(4.41E-2)†	4.1028(8.65E-2)†
DC2-DTLZ1	3	**1.1610(5.15E-4)**	╲	╲	╲	╲	╲
	5	**1.5781(2.15E-4)**	╲	╲	╲	╲	╲
	8	**2.1386(—)**	╲	╲	╲	╲	╲
	10	**2.5929(2.20E-5)**	╲	╲	╲	╲	╲
	15	**4.1422(—)**	╲	╲	╲	╲	╲
DC2-DTLZ3	3	**0.7377(3.68E-2)**	╲	╲	╲	╲	╲
	5	**1.3087(7.23E-2)**	╲	╲	╲	╲	╲
	8	**2.0013(—)**	╲	╲	╲	╲	╲
	10	**2.5101(—)**	╲	╲	╲	╲	╲
	15	**4.0832(—)**	╲	╲	╲	╲	╲
DC3-DTLZ1	3	**1.2134(1.10E-5)**	0.0000(0.00E+0)†	0.0000(0.00E+0)†	0.0000(0.00E+0)†	0.0000(0.00E+0)†	0.0000(0.00E+0)†
	5	**1.4751(2.53E-3)**	0.0000(0.00E+0)†	0.0000(0.00E+0)†	0.0000(0.00E+0)†	0.0000(0.00E+0)†	0.0000(0.00E+0)†
	8	**1.9429(1.94E+0)**	0.0000(0.00E+0)†	0.0000(0.00E+0)†	0.0000(0.00E+0)†	0.0000(0.00E+0)†	0.0000(0.00E+0)†
	10	**2.3933(1.05E-1)**	0.0000(0.00E+0)†	0.0000(0.00E+0)†	0.0000(0.00E+0)†	0.0000(0.00E+0)†	0.0000(0.00E+0)†
	15	**4.0012(4.32E-2)**	0.0000(0.00E+0)†	0.0000(0.00E+0)†	0.0000(0.00E+0)†	0.0000(0.00E+0)†	0.0000(0.00E+0)†
DC3-DTLZ3	3	**0.6298(4.74E-2)**	0.0000(0.00E+0)†	0.0000(0.00E+0)†	0.0000(0.00E+0)†	0.0000(0.00E+0)†	0.0000(0.00E+0)†
	5	**1.1880(2.35E-2)**	0.0000(0.00E+0)†	0.0000(0.00E+0)†	0.0000(0.00E+0)†	0.0000(0.00E+0)†	0.0000(0.00E+0)†
	8	**1.7614(9.28E-2)**	0.0000(0.00E+0)†	0.0000(0.00E+0)†	0.0000(0.00E+0)†	0.0000(0.00E+0)†	0.0000(0.00E+0)†
	10	**2.3748(6.13E-2)**	0.0000(0.00E+0)†	0.0000(0.00E+0)†	0.0000(0.00E+0)†	0.0000(0.00E+0)†	0.0000(0.00E+0)†
	15	**4.1326(1.28E-2)**	0.0000(0.00E+0)†	0.0000(0.00E+0)†	0.0000(0.00E+0)†	0.0000(0.00E+0)†	0.0000(0.00E+0)†

† denotes the performance of C-TAEA is significantly better than the other peers according to the Wilcoxon's rank sum test at a 0.05 significance level; ‡ denotes the corresponding algorithm significantly outperforms C-TAEA. ╲ denotes the median metric value is not available, while — denotes the IQR is not available.

Table 8: Comparison results on IGD and HV metrics (median and IQR) for C-TAEA and the two variants on C-DTLZ Benchmark Suite

	m	IGD			HV		
		C-TAEA	Variant-I	Variant-II	C-TAEA	Variant-I	Variant-II
C1-DTLZ1	3	**2.069E-2(1.33E-5)**	2.069E-2(1.52E-4)	2.069E-2(4.83E-2)	1.3042(1.01E-3)	1.3043(3.59E-2)	**1.3045(7.86E-3)**
	5	5.278E-2(1.16E-3)	**5.272E-2(2.41E-5)**	5.279E-2(2.73E-3)	**1.5791(7.28E-4)**	1.5789(3.70E-2)	1.5790(2.94E-2)
	8	**9.912E-2(1.60E-3)**	9.914E-2(4.64E-4)	9.912E-2(2.14E-2)	2.1435(3.02E-3)	**2.1441(7.62E-2)**	2.1434(9.44E-3)
	10	1.061E-1(3.82E-3)	1.061E-1(8.93E-6)	**1.060E-1(1.15E-2)**	2.5937(2.01E-6)	2.5935(3.60E-2)	**2.5937(5.32E-4)**
	15	2.233E-1(8.02E-4)	**2.232E-1(2.07E-4)**	2.234E-1(1.57E-2)†	**4.1022(3.83E-2)**	4.1022(3.29E-2)	4.1021(1.33E-2)
C1-DTLZ3	3	**5.661E-2(8.49E-3)**	5.669E-2(3.36E-4)	9.002E+0(9.51E-3)†	**0.7351(4.00E-2)**	0.7351(1.79E-2)	0.0000(0)†
	5	5.365E-1(9.03E-1)	**5.364E-1(9.48E-3)**	1.032E+1(2.99E-2)†	0.1761(1.76E-1)	**0.1762(1.51E-3)**	0.0000(0)†
	8	**4.115E-1(1.31E-2)**	4.121E-1(3.56E-4)	1.202E+1(1.05E-3)†	**1.5943(8.54E-2)**	1.5942(6.39E-3)	0.0000(0)†
	10	**3.896E-1(8.75E-2)**	3.898E-1(8.03E-4)	5.234E+0(3.52E-2)†	**2.5132(6.34E-1)**	2.5132(1.28E-2)	0.0000(0)†
	15	8.749E-1(3.16E-2)	**8.746E-1(3.29E-4)**	1.203E+1(2.69E-2)†	**2.1825(3.86E-2)**	2.1825(6.21E-3)	0.0000(0)†
C2-DTLZ2	3	1.594E-2(2.95E-3)	2.622E-2(7.97E-5)†	**1.593E-2(1.21E-3)**	0.4131(2.81E-4)	0.3946(2.81E-4)†	**0.4163(2.81E-4)**
	5	3.386E-1(1.46E-1)	3.433E-1(1.66E-3)†	**3.378E-1(1.92E-3)**	**0.8607(2.50E-1)**	0.8151(2.50E-1)†	0.8523(2.50E-1)
	8	**1.310E-4(8.22E-4)**	1.772E-3(2.84E-4)†	1.320E-4(2.83E-3)	**1.1426(6.57E-3)**	1.1279(6.57E-3)†	1.1418(6.57E-3)
	10	**2.600E-5(1.03E-6)**	3.182E-2(3.04E-4)†	2.602E-5(3.79E-3)	**1.5937(2.70E-5)**	1.5323(2.70E-5)†	1.5933(2.70E-5)
	15	**5.657E-1(3.77E-3)**	7.128E-1(1.74E-4)†	5.858E-1(2.38E-3)†	**2.4033(6.90E-2)**	2.3895(6.90E-2)†	2.3937(6.90E-2)
C3-DTLZ1	3	**4.310E-2(1.22E-4)**	4.311E-2(3.09E-4)	4.311E-2(2.77E-2)	1.1515(5.15E-4)	**1.1558(5.15E-4)**	1.1543(5.15E-4)
	5	**1.072E-1(3.06E-5)**	1.073E-1(5.47E-8)	1.073E-1(2.68E-2)	**1.5781(2.15E-4)**	1.5747(2.15E-4)	1.5728(2.15E-4)
	8	1.993E-1(8.34E-3)	**1.992E-1(3.14E-4)**	1.994E-1(2.54E-2)	**2.1386(5.66E-4)**	2.1374(5.66E-4)	2.1365(5.66E-4)
	10	**2.103E-1(2.27E-4)**	2.103E-1(2.96E-4)	2.105E-1(4.22E-2)	**2.5929(2.20E-5)**	2.5895(2.20E-5)	2.5871(2.20E-5)
	15	**3.461E-1(4.76E-3)**	3.463E-1(3.16E-4)	3.462E-1(2.99E-2)	4.1422(3.68E-1)	**4.1467(3.68E-1)**	4.1466(3.68E-1)
C3-DTLZ4	3	4.790E-1(2.00E-6)	**4.789E-1(3.13E-4)**	4.790E-1(1.65E-2)	8.4280(1.23E-2)	8.4288(5.15E-4)	**8.4323(5.15E-4)**
	5	4.170E-1(5.51E-4)	**4.170E-1(3.99E-4)**	4.171E-1(3.55E-2)	49.5453(2.20E-3)	**49.5454(2.15E-4)**	49.5405(2.15E-4)
	8	**5.048E-1(4.77E-4)**	5.049E-1(2.70E-4)	5.051E-1(2.39E-2)	**546.4971(4.56E-2)**	546.3012(5.66E-4)	546.3991(5.66E-4)
	10	**5.604E-1(3.19E-3)**	5.604E-1(3.56E-4)	5.605E-1(1.20E-2)	**2654.4042(9.19E-2)**	2653.1089(2.20E-5)	2652.4060(2.20E-5)
	15	**7.587E-1(5.23E-3)**	7.587E-1(1.54E-4)	7.588E-1(3.87E-2)	136802.2201(3.70E-2)	**136802.2246(3.68E-1)**	136802.2203(3.68E-1)

† denotes the performance of C-TAEA is significantly better than the other peers according to the Wilcoxon's rank sum test at a 0.05 significance level; ‡ denotes the corresponding algorithm significantly outperforms C-TAEA.

4 Comparisons with Two Variants

This section provides the comparison results of the IGD and HV values obtained by C-TAEA and its two variants introduced in Section V-C of the paper. Please find the detailed information from Table 8 and Table 9.

5 Problem Formulation of the Water Distribution Network Optimization

This section briefly describes the problem formulation of the water distribution network (WDN) design, including the objective and constraint functions, used in our case study. In particular, there are four objective functions and two constraint functions in total.

5.0.1 Cost

One of the most important objective functions of the WDN design is the cost. There are many different cost metrics available in the literature. This paper considers the following form:

$$f_{cost} = C_c + C_o, \tag{17}$$

where C_c is the capital cost which accounts for the costs of network components such as pipes, storage tanks; while C_o is the operating cost which measure the energy costs for pump operation. More detailed information and configurations of the costs of pipes, storage tanks and pump operation used in the WDN model, i.e., Anytown model, can be found in [31].

Table 9: Comparison results on IGD and HV metrics (median and IQR) for C-TAEA and the two variants on DC-DTLZ Benchmark Suite

	m	IGD			HV		
		C-TAEA	Variant-I	Variant-II	C-TAEA	Variant-I	Variant-II
DC1-DTLZ1	3	5.638E-2(8.10E-5)	2.566E-1(2.31E-4)†	**5.637E-2(7.34E-5)**	1.2006(1.70E-2)	1.1910(1.70E-2)†	**1.2047(5.15E-4)**
	5	7.301E-2(3.76E-3)	7.938E-2(2.17E-4)†	**7.300E-2(5.43E-3)**	1.4783(3.27E-2)	1.4725(3.27E-2)†	**1.4799(2.15E-4)**
	8	**1.086E-1(6.44E-4)**	1.332E-1(3.40E-4)†	1.086E-1(4.16E-4)	**1.9347(8.57E-2)**	1.9266(8.57E-2)†	1.9241(5.66E-4)
	10	**1.189E-1(2.84E-3)**	1.530E-1(1.62E-4)†	1.189E-1(2.47E-3)	**2.3890(3.67E-3)**	2.3828(3.67E-3)†	2.3827(2.20E-5)
	15	**1.753E-1(1.83E-2)**	4.666E-1(1.10E-4)†	1.753E-1(3.35E-3)	**4.1012(1.73E-2)**	4.0949(1.73E-2)†	4.0908(3.68E-1)
DC1-DTLZ3	3	1.466E-1(7.62E-4)	2.393E-1(7.19E-5)†	**1.443E-1(4.92E-3)**	**0.6339(6.51E-2)**	0.6019(1.70E-2)†	0.6334(6.51E-2)
	5	2.081E-1(2.54E-3)	3.980E-1(4.72E-4)†	**2.062E-1(3.18E-3)**	1.2656(3.68E-2)	1.2249(3.27E-2)†	**1.2657(3.68E-2)**
	8	**3.401E-1(8.35E-5)**	3.635E-1(1.85E-4)†	3.404E-1(7.42E-3)	1.9829(5.39E-2)	1.8770(8.57E-2)†	**1.9830(5.39E-2)**
	10	**3.884E-1(3.18E-3)**	7.692E-1(4.61E-4)†	3.886E-1(2.94E-4)	**2.5181(6.01E-2)**	2.5103(3.67E-3)†	2.5179(6.01E-2)
	15	8.009E-1(5.10E-3)	1.609E+0(3.57E-4)†	**8.008E-1(4.18E-3)**	**4.1700(7.56E-2)**	4.0690(1.73E-2)†	4.1689(7.56E-2)
DC2-DTLZ1	3	**2.199E-2(8.44E-3)**	2.599E-1(3.00E-5)	1.732E+1(9.01E-3)†	**1.1610(5.15E-4)**	1.1609(5.15E-4)	0.0000(0)†
	5	**5.371E-2(3.07E-2)**	5.638E-1(3.94E-4)	1.126E+1(2.26E-2)†	**1.5781(2.15E-4)**	1.5753(2.15E-4)	0.0000(0)†
	8	**9.937E-2(—)**	9.936E-1(1.13E-3)	＼	**2.1396(—)**	2.1340(5.66E-4)	＼
	10	**1.048E-1(8.65E-3)**	1.147E-1(1.64E-4)	＼	**2.5931(2.15E-5)**	2.5928(2.20E-5)	＼
	15	**2.308E-1(—)**	2.310E-1(8.93E-4)	＼	4.1422(—)	**4.1441(3.68E-1)**	＼
DC2-DTLZ3	3	**5.498E-2(6.78E-2)**	5.513E-2(5.81E-4)	＼	0.7377(3.68E-2)	**0.7384(5.15E-4)**	＼
	5	**1.667E-1(9.36E-3)**	1.689E+0(—)	＼	1.3087(7.23E-2)	**1.3117(—)**	＼
	8	5.674E+1(—)	**3.723E-1(—)**	＼	**2.0013(—)**	2.0010(—)	＼
	10	**3.836E-1(—)**	3.878E-1(—)	＼	2.5101(—)	**2.5130(—)**	＼
	15	**7.959E-1(—)**	7.960E-1(9.08E-4)	＼	4.0832(—)	**4.0855(3.68E-1)**	＼
DC3-DTLZ1	3	**5.034E-2(1.72E-4)**	5.512E-2(4.27E-4)†	9.641E+0(2.58E-1)†	**1.2134(1.10E-5)**	1.2104(1.70E-2)†	0.0000(0)†
	5	**8.554E-1(1.29E-3)**	8.652E-1(1.46E-4)†	1.838E+0(1.52E+0)†	**1.4751(2.53E-3)**	1.4677(3.27E-2)†	0.0000(0)†
	8	**1.250E-1(6.01E-1)**	1.645E-1(6.28E-3)†	1.258E-1(8.77E+1)	**1.9438(8.57E-2)**	1.9347(8.57E-2)†	0.0000(0)†
	10	**2.332E-1(5.29E-3)**	2.401E-1(3.64E-4)†	1.369E+0(8.63E-1)†	**2.3933(1.05E-1)**	2.3872(3.67E-3)†	0.0000(0)†
	15	**1.837E-1(3.43E-5)**	1.858E-1(1.76E-4)†	2.521E+0(4.76E+1)†	**4.0012(4.32E-2)**	4.0001(1.73E-2)†	0.0000(0)†
DC3-DTLZ3	3	**1.250E-1(8.04E-4)**	1.334E-1(1.14E-4)†	3.322E+1(3.94E+0)†	**0.6298(4.74E-2)**	0.6208(1.70E-2)†	0.0000(0)†
	5	**2.219E-1(9.16E-3)**	2.309E-1(1.87E-4)†	3.286E+1(1.66E-2)†	**1.1880(2.35E-2)**	1.1834(3.27E-2)†	0.0000(0)†
	8	**3.374E-1(8.37E-2)**	3.512E-1(9.77E-4)†	3.429E-1(1.37E+1)†	**1.7614(9.28E-2)**	1.7531(8.57E-2)†	0.0000(0)†
	10	**3.835E-1(1.16E-3)**	3.871E-1(3.38E-4)†	5.701E+1(1.33E-1)†	**2.3748(6.13E-2)**	2.3739(3.67E-3)†	0.0000(0)†
	15	**7.872E-1(2.33E-2)**	7.893E-1(1.03E-4)†	1.580E+1(8.38E-1)†	**4.1326(1.28E-2)**	4.1325(1.73E-2)†	0.0000(0)†

† denotes the performance of C-TAEA is significantly better than the other peers according to the Wilcoxon's rank sum test at a 0.05 significance level; ‡ denotes the corresponding algorithm significantly outperforms C-TAEA. \ denotes the median metric value is not available, while — denotes the IQR is not available.

5.0.2 Resilience index

The concept of resilience index was introduced by Todini [32] to account for the reliability and availability under certain stressed conditions. Specifically, it is calculated as:

$$f_r = \frac{\sum_{j=1}^{N_n} Q_j(H_j - H_j^{min})}{\left(\sum_{k=1}^{N_r} Q_k \overline{H}_k + \sum_{i=1}^{N_p} P_i/\gamma\right) - \sum_{j=1}^{N_n} Q_j H_j}, \tag{18}$$

where Q_j and H_j are respectively the demand and head at j-th node, N_n is the number of nodes. $H_j^{\min}$ is the required head at the j-th node. γ is the specific weight of water, Q_k and $\overline{H}_k$ are discharge and the head of the k-th reservoir, N_r is the number of reservoirs. P_i is the power introduced into the network by the i-th pump and N_p is the number of pumps.

5.0.3 Statistical flow entropy

This objective function was proposed in [33], and it is formulated as:

$$f_e = S_0 + \sum_{i=1}^{N_n} F_i S_i, \tag{19}$$

where F_i is the fraction of the total flow that a network supplies to the i-th node; S_0 is entropy of sources or external supplies; S_i is the entropy of the i-th node. Specifically, they are calculated as:

$$\begin{aligned} S_0 &= -\sum_{i \in I} \frac{F_{0,i}}{Q} ln\left(\frac{F_{0,i}}{Q}\right), \\ S_i &= -\frac{Q_i}{T_i} ln\left(\frac{Q_i}{T_i}\right) - \sum_{i=1}^{N_n} \sum_{j \in N_i} \frac{F_{i,j}}{Q_i} ln\left(\frac{F_{ij}}{Q_i}\right), \end{aligned} \tag{20}$$

where $F_{0,i}$ is the inflow at the i-th source node, Q is the total demand for all nodes, and the set I includes all the source nodes. Q_i is the demand at the i-th node, while T_i is the total flow that reaches the i-th node. N_i is the set of nodes with pipes flow from the i-th node; $F_{i,j}$ is the volume flow rate in the pipe between the i-th and j-th nodes.

5.0.4 Water age

Water quality problems in a WDN often arise from interactions between water within the pipe and the pipe wall in addition to within the bulk water of storage tanks. There is a great chance for contamination and thus harm the health if the water stays in the system for a long period of time. In this case, we can see that the time required for the water to reach the customer from water sources through the network influences the water quality. As discussed in [34], water age at a demand node is used as an indicator of water quality and is defined as the average travel time from water sources to the demand nodes. Specifically, it is calculated as:

$$f_{age} = \max_{i,t}(WA_{i,t}) \tag{21}$$

where $WA_{i,t}$ indicates the water age of the i-th node at time step t and it can be calculated by EPANET [35],

5.0.5 Constraints

The first constraint considered in this paper is the satisfaction of the minimum specified pressure supplied to each node. It is formulated as:

$$H_i \geq H_i^{min}, i = 1, ..., N_n \tag{22}$$

where H_i is the pressure at the i-th node; while H_i^{min} is its corresponding minimum required pressure; N_n is the number of demand nodes.
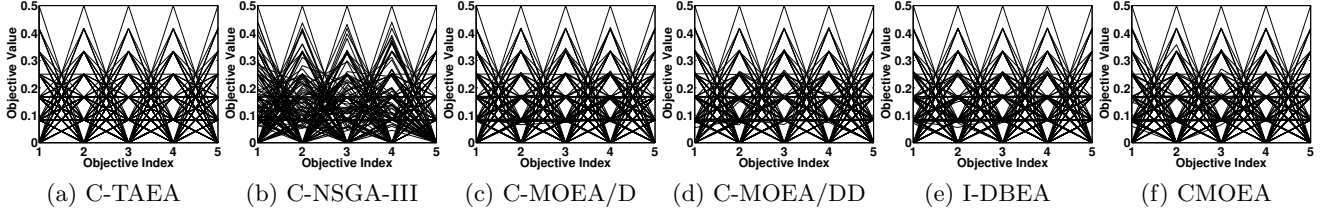
(a) C-TAEA   (b) C-NSGA-III   (c) C-MOEA/D   (d) C-MOEA/DD   (e) I-DBEA   (f) CMOEA

Figure 8: PCPs of the populations obtained by C-TAEA and the peer algorithms on 5-objective C1-DTLZ1 (median IGD value).

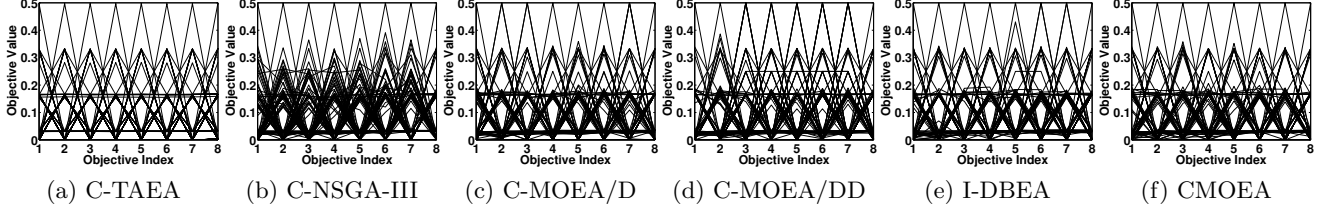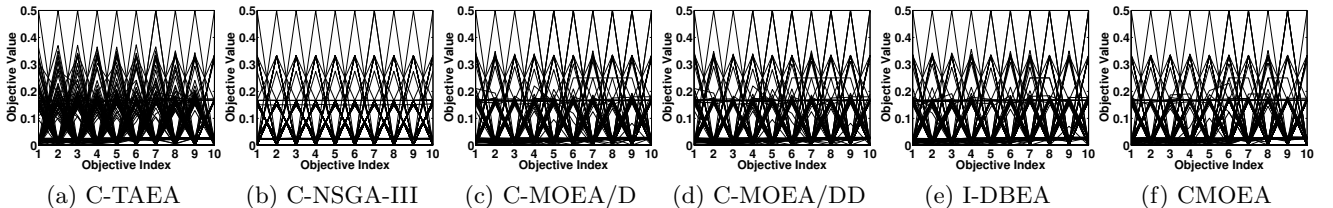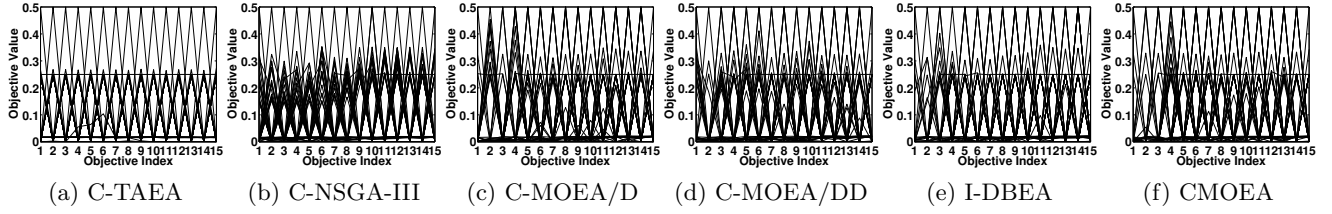(a) C-TAEA   (b) C-NSGA-III   (c) C-MOEA/D   (d) C-MOEA/DD   (e) I-DBEA   (f) CMOEA

Figure 9: PCPs of the populations obtained by C-TAEA and the peer algorithms on 8-objective C1-DTLZ1 (median IGD value).

Moreover, the height of water in a storage tank is required to be recovered over a normal operating cycle. In other words, the volume of water in a storage tank at the end of a day must be no less than the volume at the beginning of a day. Specifically, the second constraint function is defined as:

$$V_{k,E} \geq V_{k,S}, k = 1, ..., N_t \tag{23}$$

where $V_{k,S}$ represents the volume of the water at the beginning of a day for the k-th tank while $V_{k,E}$ represents the corresponding volume at the end of a day. N_t is the number of storage tanks in a WDN.

Note that all the above mentioned objective and constraint functions are calculated by EPANET [35]. It is a software developed by the United States Environmental Protection Agency, and is used to model the hydraulic and water quality behavior of water distribution piping systems. In particular, EPANET is able to simulate: 1) the flow of water in each pipe; 2) the pressure at each node; 3) the height of the water in each tank; and 4) water age.

6 Plots of populations

In this section, we show the parallel coordinate plots (PCPs) of the populations obtained by C-TAEA and the peer algorithms on different test instances from 5-objective to 15-objective cases. Here the population used in our plots is the one having the median IGD value. In particular, we only plot the non-dominated solutions.

(a) C-TAEA   (b) C-NSGA-III   (c) C-MOEA/D   (d) C-MOEA/DD   (e) I-DBEA   (f) CMOEA

Figure 10: PCPs of the populations obtained by C-TAEA and the peer algorithms on 10-objective C1-DTLZ1 (median IGD value).
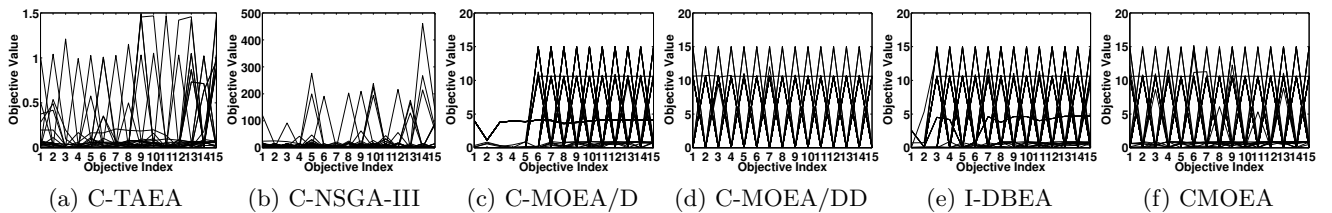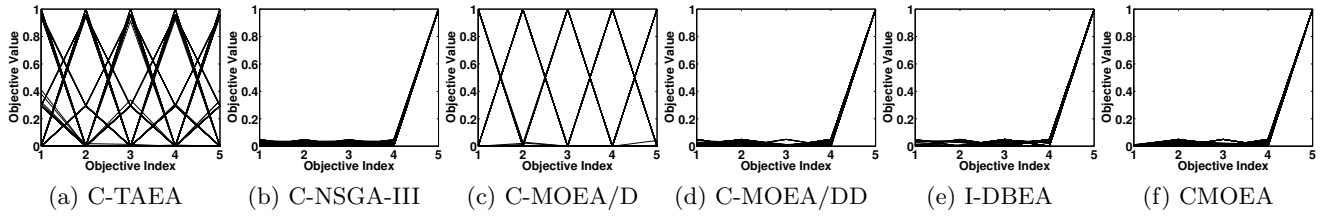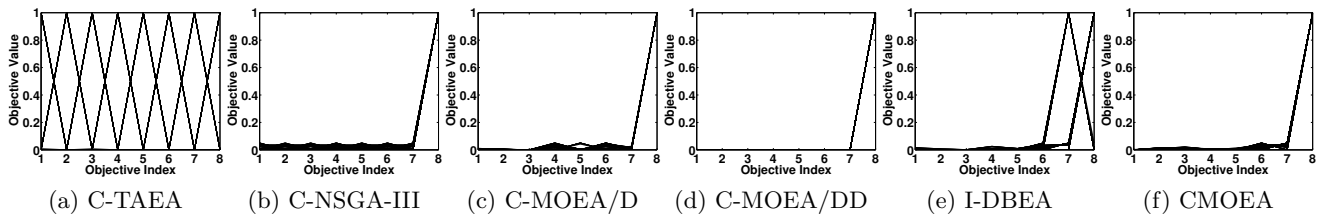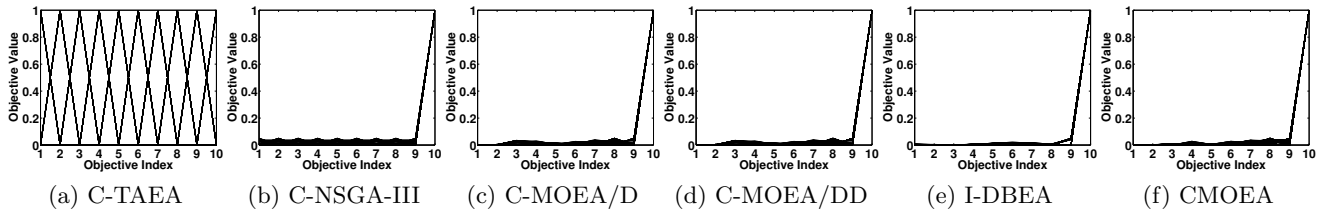
(a) C-TAEA   (b) C-NSGA-III   (c) C-MOEA/D   (d) C-MOEA/DD   (e) I-DBEA   (f) CMOEA

Figure 11: PCPs of the populations obtained by C-TAEA and the peer algorithms on 15-objective C1-DTLZ1 (median IGD value).

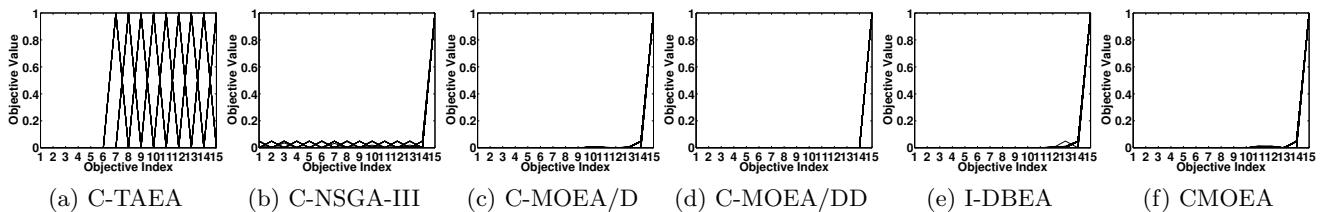(a) C-TAEA   (b) C-NSGA-III   (c) C-MOEA/D   (d) C-MOEA/DD   (e) I-DBEA   (f) CMOEA
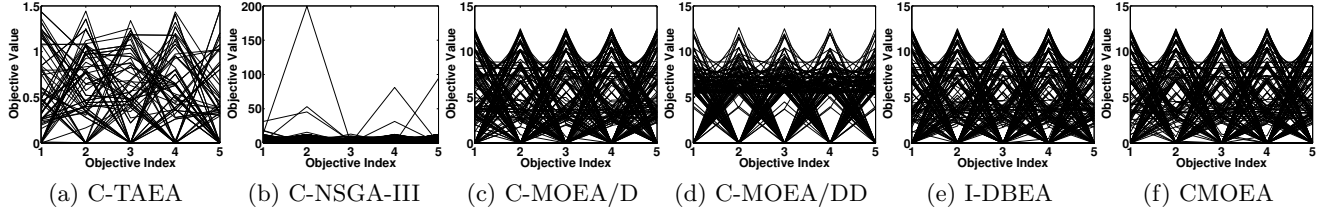
Figure 12: PCPs of the populations obtained by C-TAEA and the peer algorithms on 5-objective C1-DTLZ3 (median IGD value).

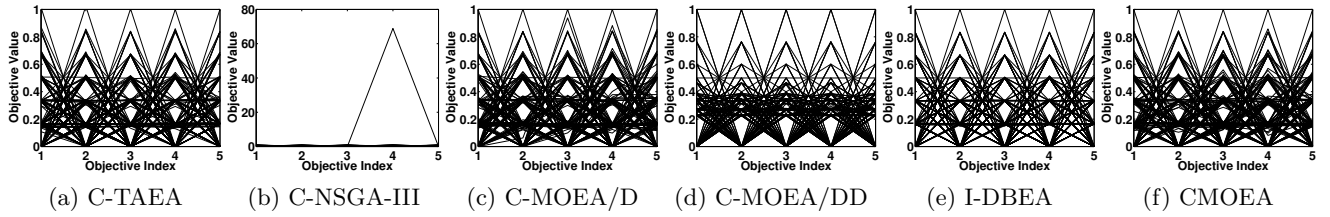(a) C-TAEA   (b) C-NSGA-III   (c) C-MOEA/D   (d) C-MOEA/DD   (e) I-DBEA   (f) CMOEA
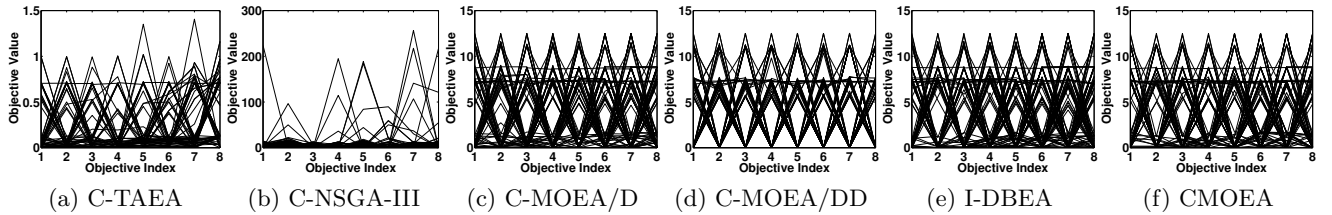
Figure 13: PCPs of the populations obtained by C-TAEA and the peer algorithms on 8-objective C1-DTLZ3 (median IGD value).

(a) C-TAEA   (b) C-NSGA-III   (c) C-MOEA/D   (d) C-MOEA/DD   (e) I-DBEA   (f) CMOEA
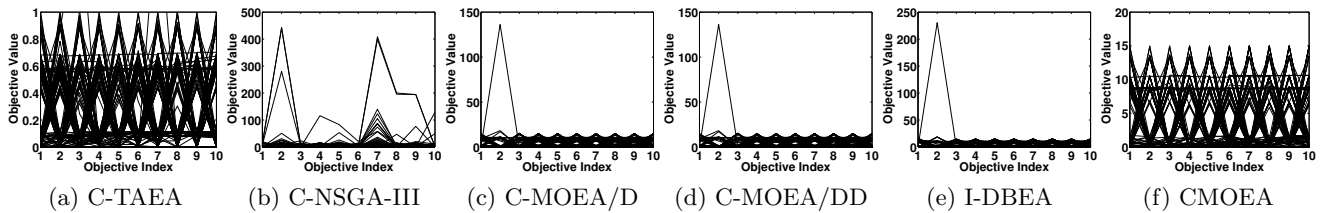
Figure 14: PCPs of the populations obtained by C-TAEA and the peer algorithms on 10-objective C1-DTLZ3 (median IGD value).
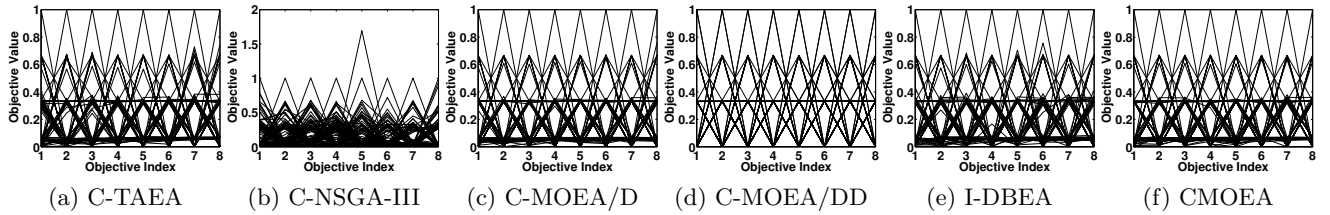

(a) C-TAEA   (b) C-NSGA-III   (c) C-MOEA/D   (d) C-MOEA/DD   (e) I-DBEA   (f) CMOEA

Figure 15: PCPs of the populations obtained by C-TAEA and the peer algorithms on 15-objective C1-DTLZ3 (median IGD value).
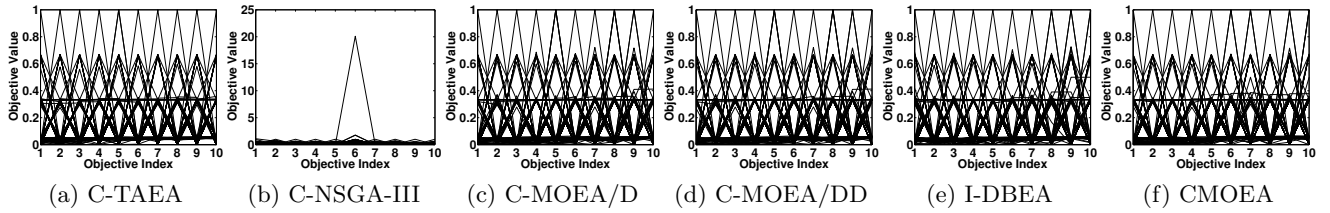
(a) C-TAEA   (b) C-NSGA-III   (c) C-MOEA/D   (d) C-MOEA/DD   (e) I-DBEA   (f) CMOEA

Figure 16: PCPs of the populations obtained by C-TAEA and the peer algorithms on 5-objective C2-DTLZ2 (median IGD value).

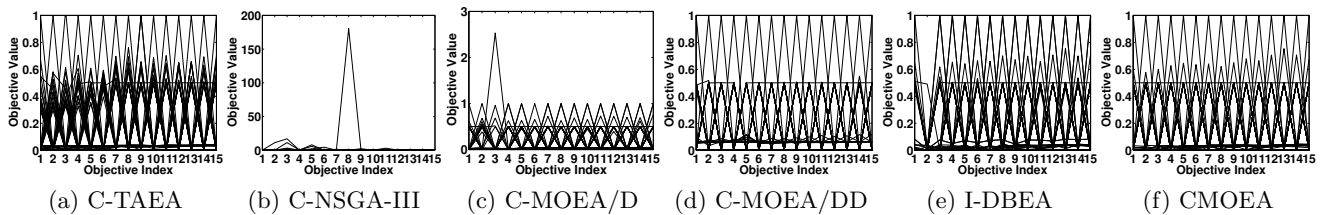(a) C-TAEA   (b) C-NSGA-III   (c) C-MOEA/D   (d) C-MOEA/DD   (e) I-DBEA   (f) CMOEA

Figure 17: PCPs of the populations obtained by C-TAEA and the peer algorithms on 8-objective C2-DTLZ2 (median IGD value).

(a) C-TAEA   (b) C-NSGA-III   (c) C-MOEA/D   (d) C-MOEA/DD   (e) I-DBEA   (f) CMOEA

Figure 18: PCPs of the populations obtained by C-TAEA and the peer algorithms on 10-objective C2-DTLZ2 (median IGD value).

(a) C-TAEA   (b) C-NSGA-III   (c) C-MOEA/D   (d) C-MOEA/DD   (e) I-DBEA   (f) CMOEA

Figure 19: PCPs of the populations obtained by C-TAEA and the peer algorithms on 15-objective C2-DTLZ2 (median IGD value).
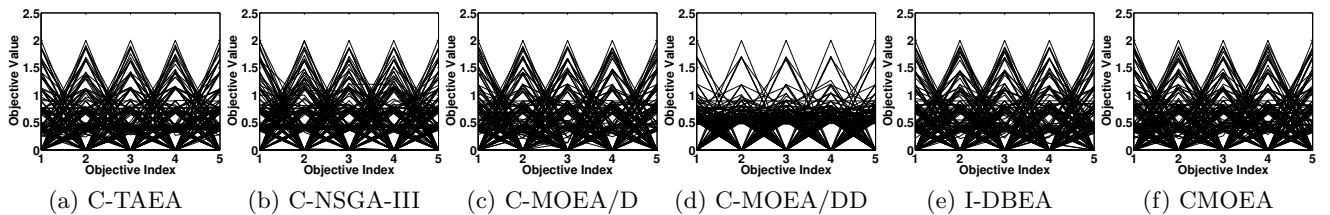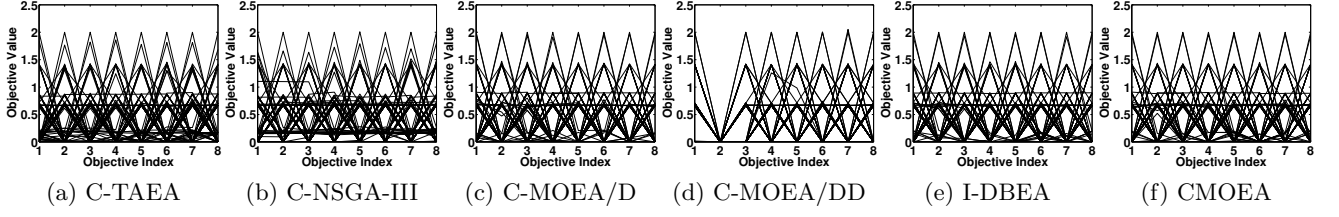
(a) C-TAEA   (b) C-NSGA-III   (c) C-MOEA/D   (d) C-MOEA/DD   (e) I-DBEA   (f) CMOEA

Figure 20: PCPs of the populations obtained by C-TAEA and the peer algorithms on 5-objective C3-DTLZ1 (median IGD value).

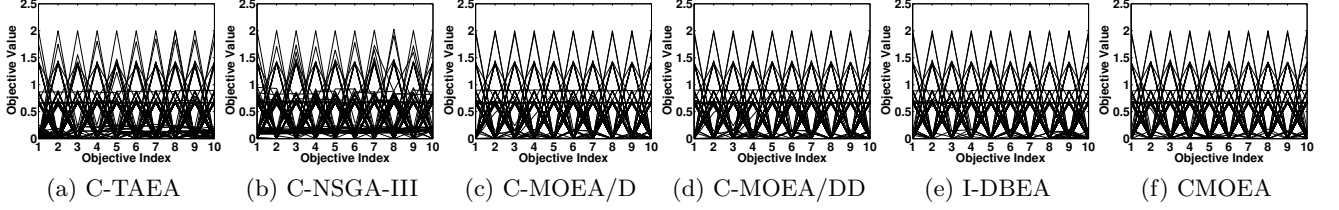(a) C-TAEA   (b) C-NSGA-III   (c) C-MOEA/D   (d) C-MOEA/DD   (e) I-DBEA   (f) CMOEA

Figure 21: PCPs of the populations obtained by C-TAEA and the peer algorithms on 8-objective C3-DTLZ1 (median IGD value).

(a) C-TAEA   (b) C-NSGA-III   (c) C-MOEA/D   (d) C-MOEA/DD   (e) I-DBEA   (f) CMOEA

Figure 22: PCPs of the populations obtained by C-TAEA and the peer algorithms on 10-objective C3-DTLZ1 (median IGD value).

(a) C-TAEA   (b) C-NSGA-III   (c) C-MOEA/D   (d) C-MOEA/DD   (e) I-DBEA   (f) CMOEA

Figure 23: PCPs of the populations obtained by C-TAEA and the peer algorithms on 15-objective C3-DTLZ1 (median IGD value).
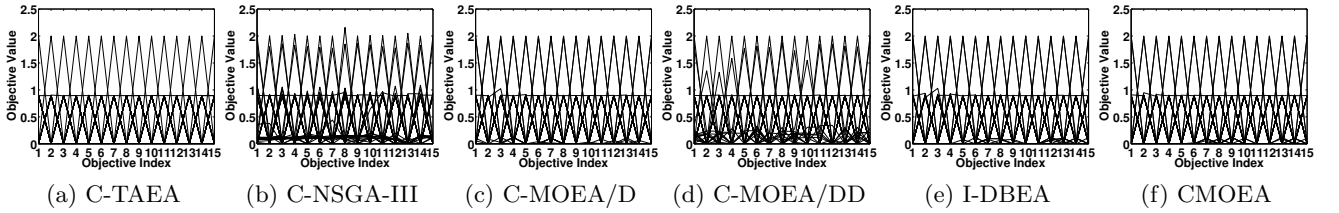

(a) C-TAEA   (b) C-NSGA-III   (c) C-MOEA/D   (d) C-MOEA/DD   (e) I-DBEA   (f) CMOEA

Figure 24: PCPs of the populations obtained by C-TAEA and the peer algorithms on 5-objective C3-DTLZ4 (median IGD value).

(a) C-TAEA (b) C-NSGA-III (c) C-MOEA/D (d) C-MOEA/DD (e) I-DBEA (f) CMOEA

Figure 25: PCPs of the populations obtained by C-TAEA and the peer algorithms on 8-objective C3-DTLZ4 (median IGD value).

(a) C-TAEA (b) C-NSGA-III (c) C-MOEA/D (d) C-MOEA/DD (e) I-DBEA (f) CMOEA

Figure 26: PCPs of the population obtained by C-TAEA and the peer algorithms on 10-objective C3-DTLZ4 (median IGD value).

(a) C-TAEA (b) C-NSGA-III (c) C-MOEA/D (d) C-MOEA/DD (e) I-DBEA (f) CMOEA

Figure 27: PCPs of the populations obtained by C-TAEA and the peer algorithms on 15-objective C3-DTLZ4 (median IGD value).

(a) C-TAEA (b) C-NSGA-III (c) C-MOEA/D (d) C-MOEA/DD (e) I-DBEA (f) CMOEA
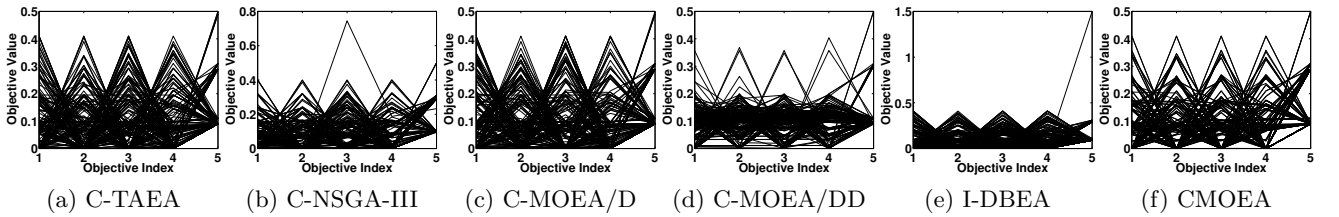
Figure 28: PCPs of the populations obtained by C-TAEA and the peer algorithms on 5-objective DC1-DTLZ1.

(a) C-TAEA (b) C-NSGA-III (c) C-MOEA/D (d) C-MOEA/DD (e) I-DBEA (f) CMOEA
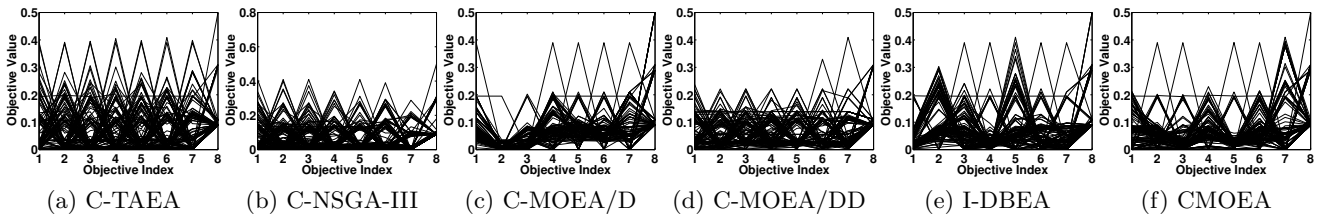
Figure 29: PCPs of the populations obtained by C-TAEA and the peer algorithms on 8-objective DC1-DTLZ1.

(a) C-TAEA   (b) C-NSGA-III   (c) C-MOEA/D   (d) C-MOEA/DD   (e) I-DBEA   (f) CMOEA
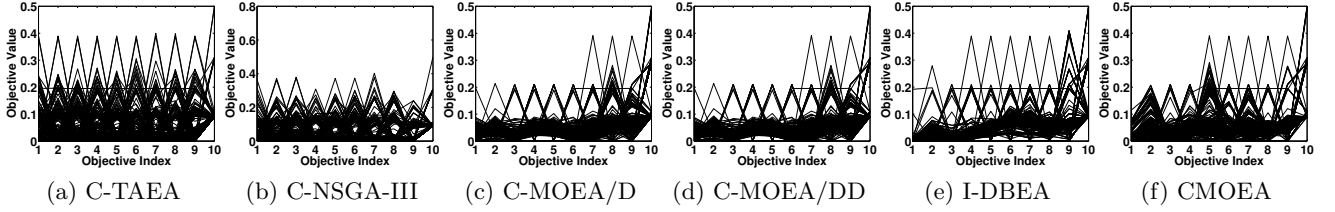
Figure 30: PCPs of the populations obtained by C-TAEA and the peer algorithms on 10-objective DC1-DTLZ1.

(a) C-TAEA   (b) C-NSGA-III   (c) C-MOEA/D   (d) C-MOEA/DD   (e) I-DBEA   (f) CMOEA
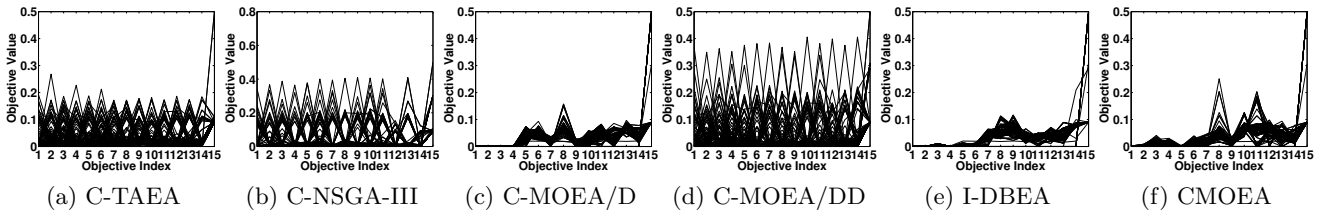
Figure 31: PCPs of the populations obtained by C-TAEA and the peer algorithms on 15-objective DC1-DTLZ1.

(a) C-TAEA (b) C-NSGA-III (c) C-MOEA/D (d) C-MOEA/DD (e) I-DBEA (f) CMOEA
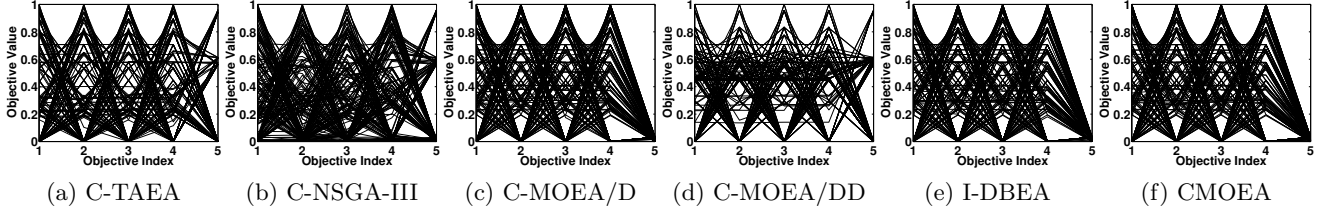
Figure 32: PCPs of the populations obtained by C-TAEA and the peer algorithms on 5-objective DC1-DTLZ3.

(a) C-TAEA (b) C-NSGA-III (c) C-MOEA/D (d) C-MOEA/DD (e) I-DBEA (f) CMOEA
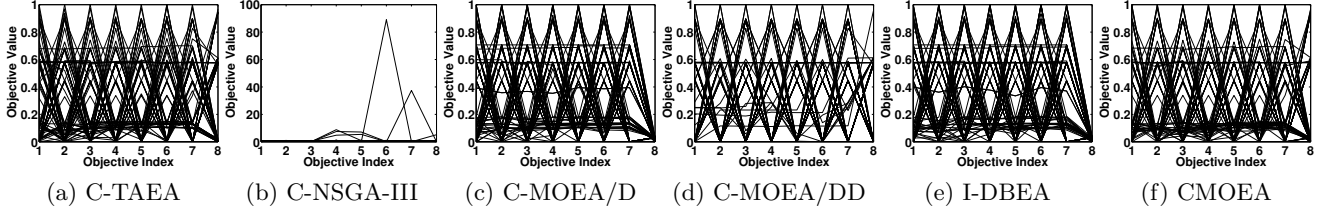
Figure 33: PCPs of the populations obtained by C-TAEA and the peer algorithms on 8-objective DC1-DTLZ3.

(a) C-TAEA (b) C-NSGA-III (c) C-MOEA/D (d) C-MOEA/DD (e) I-DBEA (f) CMOEA
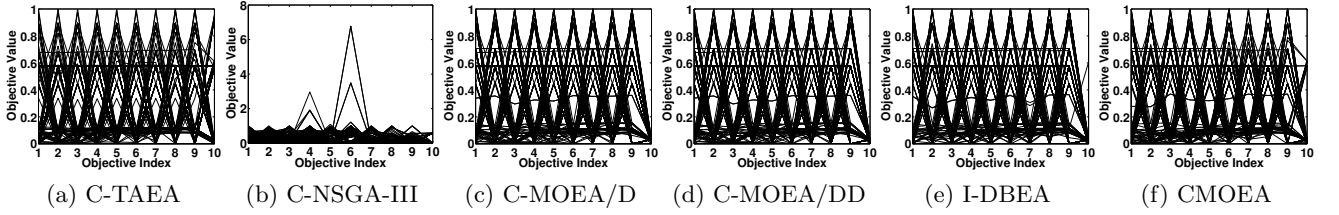
Figure 34: PCPs of the populations obtained by C-TAEA and the peer algorithms on 10-objective DC1-DTLZ3.

(a) C-TAEA (b) C-NSGA-III (c) C-MOEA/D (d) C-MOEA/DD (e) I-DBEA (f) CMOEA
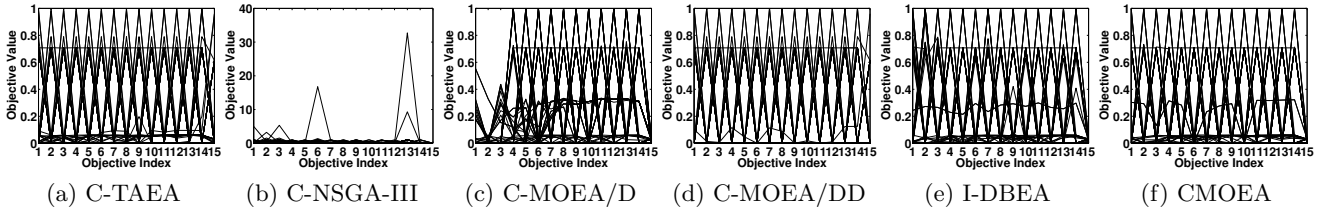
Figure 35: PCPs of the populations obtained by C-TAEA and the peer algorithms on 15-objective DC1-DTLZ3.

(a) C-TAEA (b) C-NSGA-III (c) C-MOEA/D (d) C-MOEA/DD (e) I-DBEA (f) CMOEA
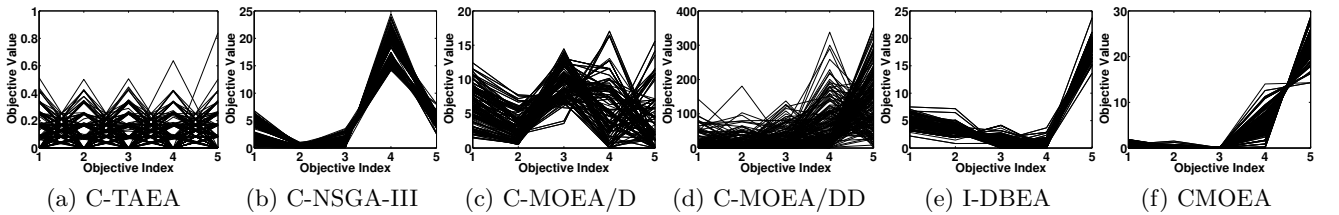
Figure 36: PCPs of the populations obtained by C-TAEA and the peer algorithms on 5-objective DC2-DTLZ1.

(a) C-TAEA   (b) C-NSGA-III   (c) C-MOEA/D   (d) C-MOEA/DD   (e) I-DBEA   (f) CMOEA
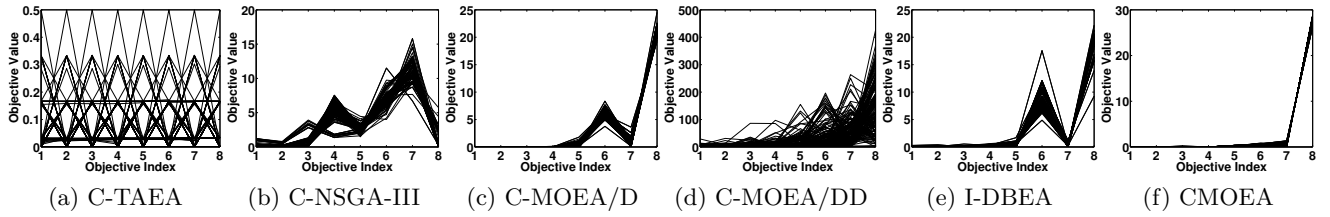
Figure 37: PCPs of the populations obtained by C-TAEA and the peer algorithms on 8-objective DC2-DTLZ1.

(a) C-TAEA   (b) C-NSGA-III   (c) C-MOEA/D   (d) C-MOEA/DD   (e) I-DBEA   (f) CMOEA
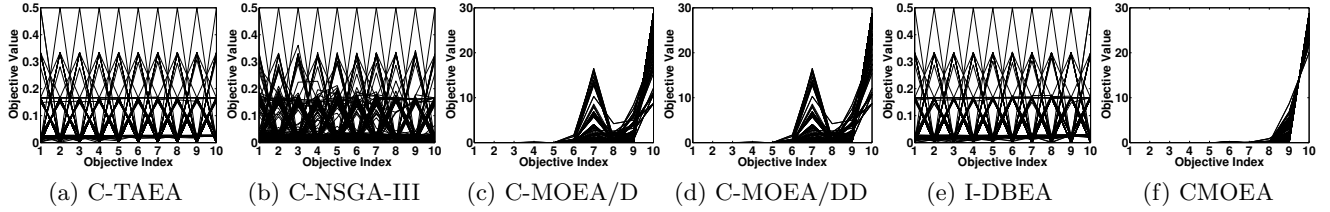
Figure 38: PCPs of the populations obtained by C-TAEA and the peer algorithms on 10-objective DC2-DTLZ1.

(a) C-TAEA   (b) C-NSGA-III   (c) C-MOEA/D   (d) C-MOEA/DD   (e) I-DBEA   (f) CMOEA
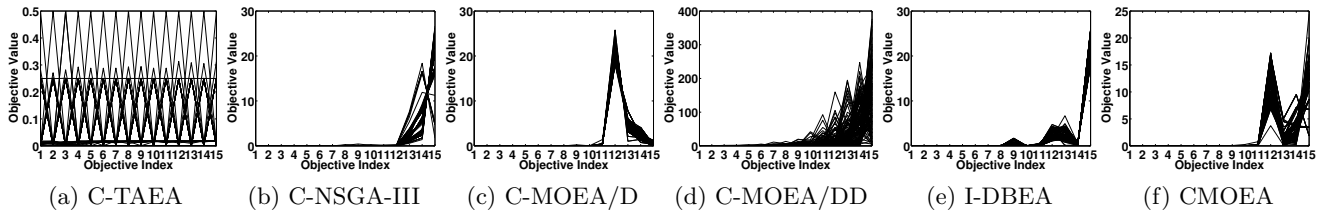
Figure 39: PCPs of the populations obtained by C-TAEA and the peer algorithms on 15-objective DC2-DTLZ1.

(a) C-TAEA   (b) C-NSGA-III   (c) C-MOEA/D   (d) C-MOEA/DD   (e) I-DBEA   (f) CMOEA
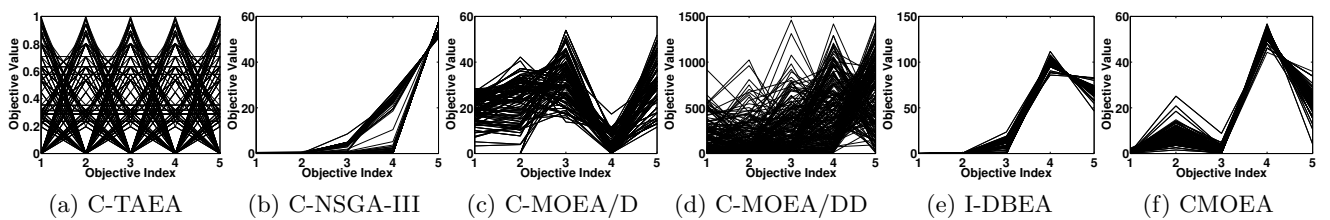
Figure 40: PCPs of the populations obtained by C-TAEA and the peer algorithms on 5-objective DC2-DTLZ3.

(a) C-TAEA   (b) C-NSGA-III   (c) C-MOEA/D   (d) C-MOEA/DD   (e) I-DBEA   (f) CMOEA
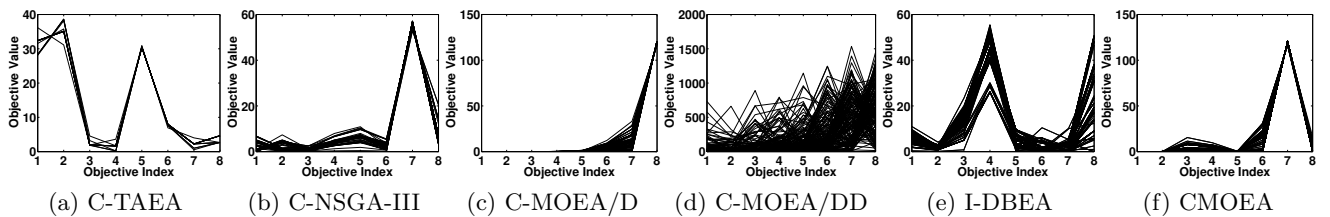
Figure 41: PCPs of the populations obtained by C-TAEA and the peer algorithms on 8-objective DC2-DTLZ3.

(a) C-TAEA   (b) C-NSGA-III   (c) C-MOEA/D   (d) C-MOEA/DD   (e) I-DBEA   (f) CMOEA
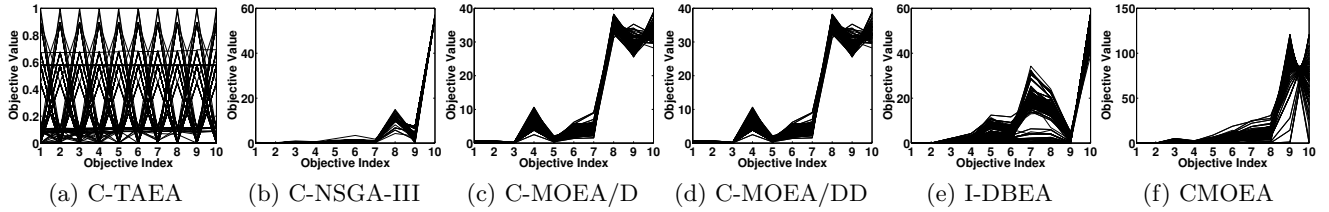
Figure 42: PCPs of the populations obtained by C-TAEA and the peer algorithms on 10-objective DC2-DTLZ3.

(a) C-TAEA   (b) C-NSGA-III   (c) C-MOEA/D   (d) C-MOEA/DD   (e) I-DBEA   (f) CMOEA
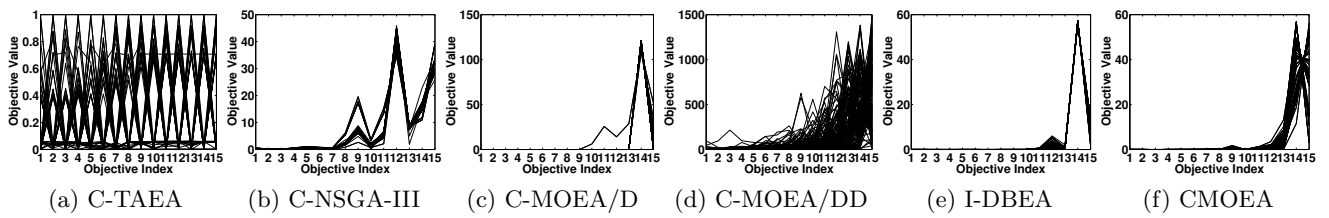
Figure 43: PCPs of the populations obtained by C-TAEA and the peer algorithms on 15-objective DC2-DTLZ3.

(a) C-TAEA   (b) C-NSGA-III   (c) C-MOEA/D   (d) C-MOEA/DD   (e) I-DBEA   (f) CMOEA
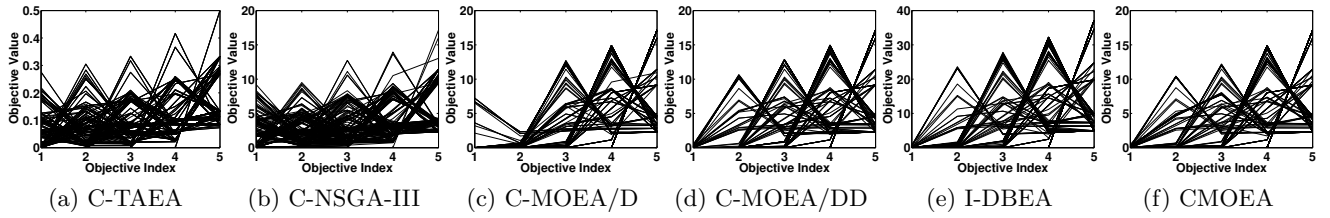
Figure 44: PCPs of the populations obtained by C-TAEA and the peer algorithms on 5-objective DC3-DTLZ1.

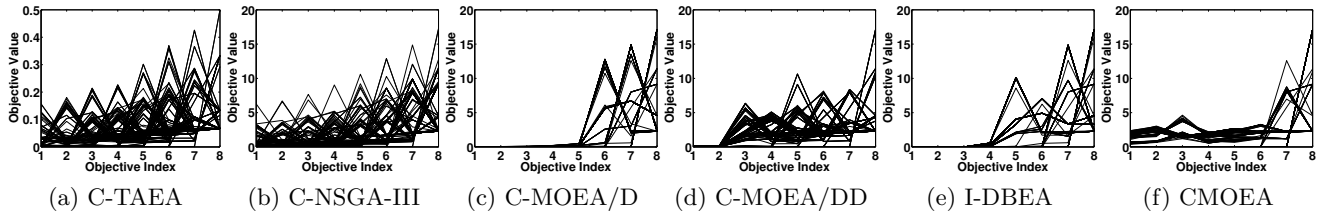(a) C-TAEA   (b) C-NSGA-III   (c) C-MOEA/D   (d) C-MOEA/DD   (e) I-DBEA   (f) CMOEA

Figure 45: PCPs of the populations obtained by C-TAEA and the peer algorithms on 8-objective DC3-DTLZ1.

Acknowledgment

References

[1] K. Deb, L. Thiele, M. Laumanns, and E. Zitzler, *Scalable Test Problems for Evolutionary Multi-objective Optimization.* London: Springer London, 2005, pp. 105–145.

[2] K. Li, J. Zheng, M. Li, C. Zhou, and H. Lv, "A novel algorithm for non-dominated hypervolume-based multiobjective optimization," in *SMC'09: Proc. of the 2009 IEEE International Conference on Systems, Man and Cybernetics*, 2009, pp. 5220–5226.

[3] K. Li, S. Kwong, R. Wang, J. Cao, and I. J. Rudas, "Multi-objective differential evolution with self-navigation," in *SMC'12: Proc. of the 2012 IEEE International Conference on Systems, Man, and Cybernetics*, 2012, pp. 508–513.

[4] K. Li, S. Kwong, J. Cao, M. Li, J. Zheng, and R. Shen, "Achieving balance between proximity and diversity in multi-objective evolutionary algorithm," *Inf. Sci.*, vol. 182, no. 1, pp. 220–242, 2012.
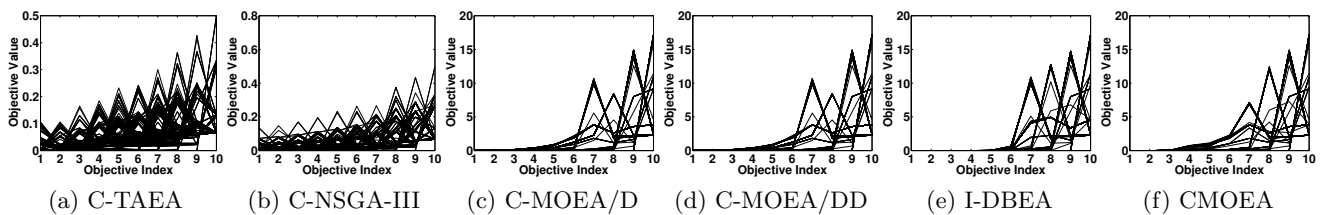
(a) C-TAEA   (b) C-NSGA-III   (c) C-MOEA/D   (d) C-MOEA/DD   (e) I-DBEA   (f) CMOEA

Figure 46: PCPs of the populations obtained by C-TAEA and the peer algorithms on 10-objective DC3-DTLZ1.

(a) C-TAEA   (b) C-NSGA-III   (c) C-MOEA/D   (d) C-MOEA/DD   (e) I-DBEA   (f) CMOEA
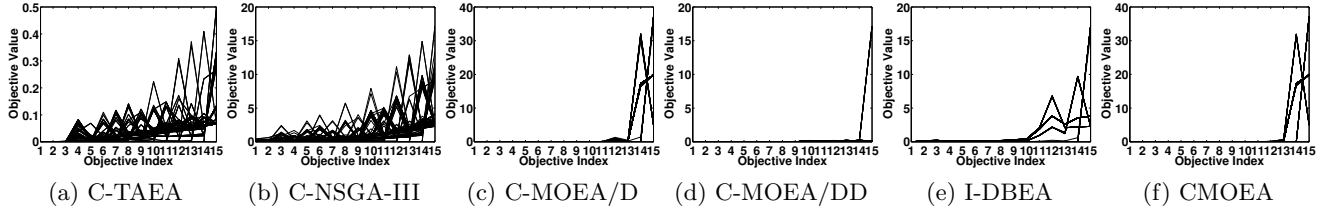
Figure 47: PCPs of the populations obtained by C-TAEA and the peer algorithms on 15-objective DC3-DTLZ1.

(a) C-TAEA   (b) C-NSGA-III   (c) C-MOEA/D   (d) C-MOEA/DD   (e) I-DBEA   (f) CMOEA
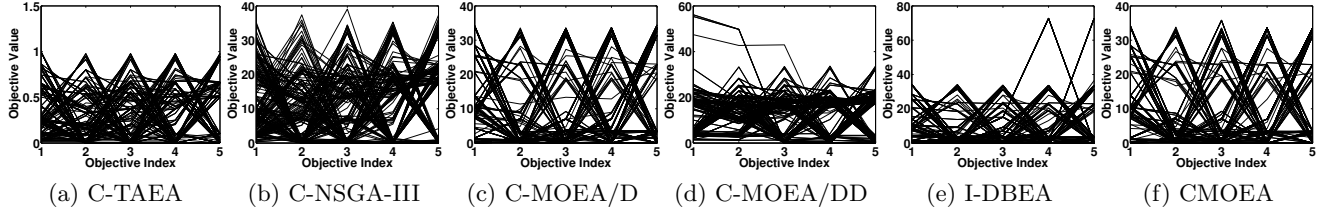
Figure 48: PCPs of the populations obtained by C-TAEA and the peer algorithms on 5-objective DC3-DTLZ3.

(a) C-TAEA   (b) C-NSGA-III   (c) C-MOEA/D   (d) C-MOEA/DD   (e) I-DBEA   (f) CMOEA
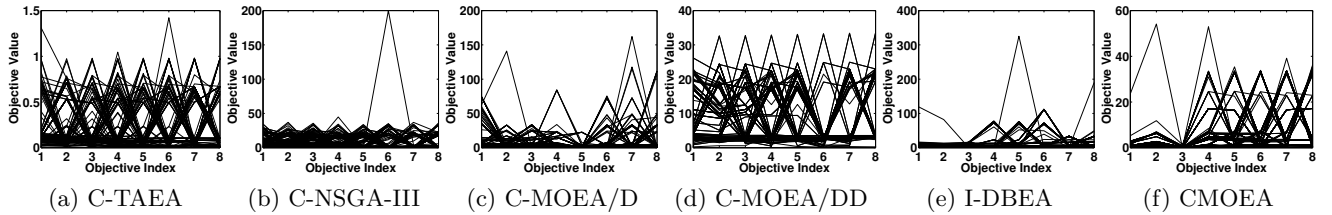
Figure 49: PCPs of the populations obtained by C-TAEA and the peer algorithms on 8-objective DC3-DTLZ3.

(a) C-TAEA   (b) C-NSGA-III   (c) C-MOEA/D   (d) C-MOEA/DD   (e) I-DBEA   (f) CMOEA
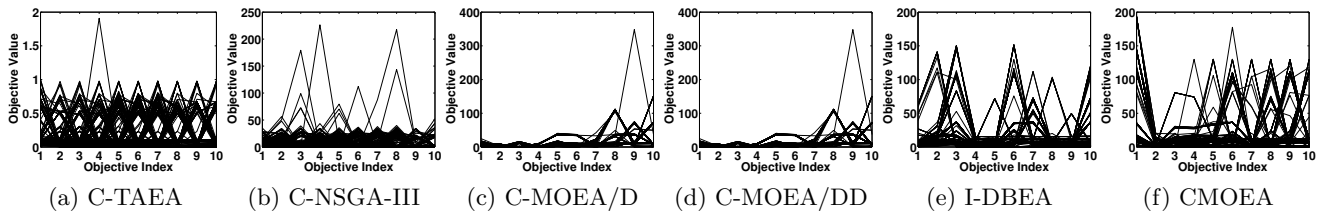
Figure 50: PCPs of the populations obtained by C-TAEA and the peer algorithms on 10-objective DC3-DTLZ3.

(a) C-TAEA   (b) C-NSGA-III   (c) C-MOEA/D   (d) C-MOEA/DD   (e) I-DBEA   (f) CMOEA

Figure 51: PCPs of the populations obtained by C-TAEA and the peer algorithms on 15-objective DC3-DTLZ3.

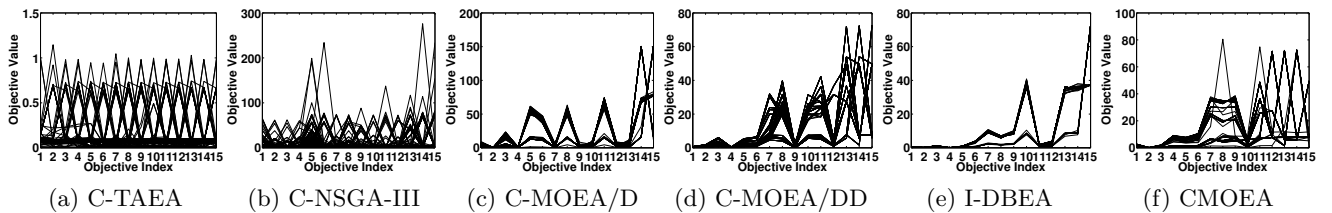[5] K. Li, S. Kwong, R. Wang, K. Tang, and K. Man, "Learning paradigm based on jumping genes: A general framework for enhancing exploration in evolutionary multiobjective optimization," *Inf. Sci.*, vol. 226, pp. 1–22, 2013.

[6] K. Li, Q. Zhang, S. Kwong, M. Li, and R. Wang, "Stable matching-based selection in evolutionary multiobjective optimization," *IEEE Trans. Evolutionary Computation*, vol. 18, no. 6, pp. 909–923, 2014.

[7] K. Li, Á. Fialho, S. Kwong, and Q. Zhang, "Adaptive operator selection with bandits for a multiobjective evolutionary algorithm based on decomposition," *IEEE Trans. Evolutionary Computation*, vol. 18, no. 1, pp. 114–130, 2014.

[8] K. Li and S. Kwong, "A general framework for evolutionary multiobjective optimization via manifold learning," *Neurocomputing*, vol. 146, pp. 65–74, 2014.

[9] M. Wu, S. Kwong, Q. Zhang, K. Li, R. Wang, and B. Liu, "Two-level stable matching-based selection in MOEA/D," in *SMC'15: Proc. of the 2015 IEEE International Conference on Systems, Man, and Cybernetics*, 2015, pp. 1720–1725.

[10] K. Li, K. Deb, and Q. Zhang, "Evolutionary multiobjective optimization with hybrid selection principles," in *CEC'15: Proc. of 2015 IEEE Congress on Evolutionary Computation*, 2015, pp. 900–907.

[11] K. Li, K. Deb, Q. Zhang, and S. Kwong, "An evolutionary many-objective optimization algorithm based on dominance and decomposition," *IEEE Trans. Evolutionary Computation*, vol. 19, no. 5, pp. 694–716, 2015.

[12] K. Li, S. Kwong, and K. Deb, "A dual-population paradigm for evolutionary multiobjective optimization," *Inf. Sci.*, vol. 309, pp. 50–72, 2015.

[13] K. Li, M. N. Omidvar, K. Deb, and X. Yao, "Variable interaction in multi-objective optimization problems," in *PPSN'16: Proc. of 14th International Conference on Parallel Problem Solving from Nature*, 2016, pp. 399–409.

[14] K. Li and K. Deb, "Performance assessment for preference-based evolutionary multi-objective optimization using reference points," COIN Report, Tech. Rep., 2016.

[15] M. Wu, S. Kwong, Y. Jia, K. Li, and Q. Zhang, "Adaptive weights generation for decomposition-based multi-objective optimization using gaussian process regression," in *GECCO'17: Proc. of the 2017 Genetic and Evolutionary Computation Conference*, 2017, pp. 641–648.

[16] K. Li, K. Deb, O. T. Altinöz, and X. Yao, "Empirical investigations of reference point based methods when facing a massively large number of objectives: First results," in *EMO'17: Proc. of the 9th International Conference on Evolutionary Multi-Criterion Optimization*, 2017, pp. 390–405.

[17] M. Wu, K. Li, S. Kwong, Y. Zhou, and Q. Zhang, "Matching-based selection with incomplete lists for decomposition multiobjective optimization," *IEEE Trans. Evolutionary Computation*, vol. 21, no. 4, pp. 554–568, 2017.

[18] K. Li, K. Deb, Q. Zhang, and Q. Zhang, "Efficient nondomination level update method for steady-state evolutionary multiobjective optimization," *IEEE Trans. Cybernetics*, vol. 47, no. 9, pp. 2838–2849, 2017.

[19] R. Chen, K. Li, and X. Yao, "Dynamic multiobjectives optimization with a changing number of objectives," *IEEE Trans. Evolutionary Computation*, vol. 22, no. 1, pp. 157–171, 2018.

[20] K. Li, K. Deb, and X. Yao, "R-metric: Evaluating the performance of preference-based evolutionary multi-objective optimization using reference points," *IEEE Trans. Evol. Comput.*, 2018, accepted for publication.

[21] K. Li, R. Chen, G. Fu, and X. Yao, "Two-archive evolutionary algorithm for constrained multi-objective optimization," *IEEE Trans. Evol. Comput.*, 2018, accepted for publication.

[22] M. Wu, K. Li, S. Kwong, Q. Zhang, and J. Zhang, "Learning to decompose: A paradigm for decomposition-based multi-objective optimization," *IEEE Trans. Evol. Comput.*, 2018, accepted for publication.

[23] K. Li, R. Chen, G. Min, and X. Yao, "Integration of preferences in decomposition-based evolutionary multi-objective optimization," *IEEE Trans. Cybernetics*, 2018, accepted for publication.

[24] H. Jain and K. Deb, "An evolutionary many-objective optimization algorithm using reference-point based nondominated sorting approach, part II: handling constraints and extending to an adaptive approach," *IEEE Trans. Evolutionary Computation*, vol. 18, no. 4, pp. 602–622, 2014.

[25] H. Li and Q. Zhang, "Multiobjective optimization problems with complicated pareto sets, MOEA/D and NSGA-II," *IEEE Trans. Evolutionary Computation*, vol. 13, no. 2, pp. 284–302, 2009.

[26] K. Deb and H. Jain, "An evolutionary many-objective optimization algorithm using reference-point-based nondominated sorting approach, part I: solving problems with box constraints," *IEEE Trans. Evolutionary Computation*, vol. 18, no. 4, pp. 577–601, 2014.

[27] M. Asafuddoula, T. Ray, and R. A. Sarker, "A decomposition-based evolutionary algorithm for many objective optimization," *IEEE Trans. Evolutionary Computation*, vol. 19, no. 3, pp. 445–460, 2015.

[28] Y. G. Woldesenbet, G. G. Yen, and B. G. Tessema, "Constraint handling in multiobjective evolutionary optimization," *IEEE Trans. Evolutionary Computation*, vol. 13, no. 3, pp. 514–525, 2009.

[29] K. Deb and R. B. Agrawal, "Simulated binary crossover for continuous search space," *Complex Systems*, vol. 9, 1994.

[30] K. Deb and M. Goyal, "A combined genetic adaptive search (GeneAS) for engineering design," *Computer Science and Informatics*, vol. 26, pp. 30–45, 1996.

[31] http://emps.exeter.ac.uk/engineering/research/cws/resources/benchmarks/expansion/anytown.php.

[32] E. Todini, "Looped water distribution networks design using a resilience index based heuristic approach," *Urban Water*, vol. 2, no. 2, pp. 115–122, 2000.

[33] S. Saleh and T. Tanyimboh, "Multi-directional maximum-entropy approach to the evolutionary design optimization of water distribution systems," *Water Resources Management*, vol. 30, no. 6, pp. 1885–1901, 2016.

[34] R. Farmani, G. Walters, and D. Savic, "Evolutionary multi-objective optimization of the design and operation of water distribution network: total cost vs. reliability vs. water quality," *Journal of Hydroinformatics*, vol. 8, no. 3, pp. 165–179, 2006.

[35] https://www.epa.gov/water-research/epanet#downloads.